use DD 250
Reports File Copy

GEORGIA INSTITUTE OF TECHNOLOGY
Engineering Experiment Station

PROJECT INITIATION

Date: September 20, 1973

Project Title: "Investigation of a Leading-Edge Antenna for an AH-1 Helicopter"

Project No.: A-1551

Project Director: Dr. D. G. Bodnar

Sponsor: U.S. Army--Frankford Arsenal; Philadelphia, Pennsylvania 19137

Effective: June 14, 1973 Estimated to run until: December 14, 1973

Type Agreement: Contract No. DAAA25-73-C-0648 Amount: $ 39,933

REPORTS REQUIRED: Monthly Accomplishment Reports; Final Technical Report; Drawings & Lists; Engineering Data

SPONSOR CONTACT PERSONS:

Technical Matters

Mr. Michael Milstead
U.S. Army-Frankford Arsenal
Tacony & Bridge Streets
Philadelphia, Pennsylvania
19137

Phone: (215) 831-5843,
Ext. 6411

Administrative Matters
(thru GTRI)

Mr. R. J. Whitcomb (ACO)
ONR Resident Representative
Campus

DEFENSE PRIORITY RATING: DO-A5 under DM5 Reg. 1.

Assigned to Sensor Systems Division

COPIES TO:

Project Director	Photographic Laboratory
Director	✓Security, Property, Reports Coordinator
Assistant Director	EES Accounting
GTRI	EES Supply Services
Division Chief(s)	Library
Service Groups	Rich Electronic Computer Center
Patent Coordinator	Project File
	Other

Report File Posted 8-28-74 B

GEORGIA INSTITUTE OF TECHNOLOGY
Engineering Experiment Station

PROJECT TERMINATION

Date May 30, 1974

PROJECT TITLE: "Investigation of a Leading-Edge Antenna for an AH-1 Helicopter"

PROJECT NO: A-1551

PROJECT DIRECTOR: D. G. Bodnar

SPONSOR: U.S. Army - Frankford Arsenal; Philadelphia, Pennsylvania

TERMINATION EFFECTIVE: April 15, 1974 (Final Report due)

CHARGES SHOULD CLEAR ACCOUNTING BY: April 30, 1974

CONTRACT CLOSEOUT ITEMS REMAINING: Final Invoice and Closing Documents
Final Report of Inventions
Government Property Inventory and Cert.

SENSOR SYSTEMS DIVISION

COPIES TO:

Project Director
Director
Associate Director
Assistant Directors
Division Chief
Branch Head
Accounting
Engineering Design Services
General Office Services
Photographic Laboratory
Purchasing
Report Section
Library
Security
Rich Electronic Computer Center

Form EES 402 (R10-62)

A-1551

ENGINEERING EXPERIMENT STATION

GEORGIA INSTITUTE OF TECHNOLOGY • ATLANTA, GEORGIA 30332

15 August 1973

Commander, Frankford Arsenal
Attention: SMUFA-N6100
Philadelphia, PA 19137

Attention: N6100

Reference: Contract No. DAAA25-73-C-0648

Subject: Monthly Technical Status Report No. 1 for the period from 14 June to 14 July 1973.

Gentlemen:

This status report covers the work performed on the referenced contract for the period from 14 June to 14 July 1973.

A notice of award dated 14 June 1973 was received by Georgia Tech. The contract, however, has not been received.

A system study phase of the program has been initiated. This phase consists of establishment of AH-1 mission parameters, radar systems concepts, and antenna system requirements and performance specifications.

Also, the antenna system preliminary design study phase has started. In part this effort has been in the area of a computer program to generate the geodesic lens dimensions and configuration.

A computer program has been used to aid in the analysis of sum and difference geodesic lens antenna radiation patterns. This information will be used to evaluate monopulse tracking in the azimuth plane.

It is required that Georgia Tech have dimensioned drawings of the "stub wings" and vibration data of the same for the AH-1 helicopter. This information will be used for antenna design and antenna performance analysis.

During the next report period it is planned that the above reported efforts continue. Also, the predicted antenna system performance analysis and overall system analysis will be initiated.

Respectfully submitted,

R. D. Gober
Assistant Project Director

Approved:

D. G. Bodnar
Project Director
Project A-1551

A-1551

5 October 1973

Commander, Frankford Arsenal
Attention: SMUFA-N6100
Philadelphia, PA 19137

Attention: N6100

Reference: Contract No. DAAA25-73-C-0648

Subject: Monthly Technical Status Report No. 2 for the period from 14 July to 13 August 1973.

Gentlemen:

This status report covers the work performed on the referenced contract for the period from 14 July to 13 August.

The computer study of widely spaced geodesic lens antennas for monopulse application was completed. When widely spaced such as would be the case of an antenna on each of the stub wings, the grating lobe radiation patterns would cause ambiguities when used for tracking. These ambiguities cannot be resolved in a practical system design.

For the above stated reason, two antennas should not be used to obtain azimuth monopulse. Instead, a single plane monopulse feed on the lens is anticipated. Two geodesic lens will be "nested" to form a single antenna assembly with multiple feeds to derive both azimuth and elevation monopulse tracking capability.

Preliminary mission parameters for the AH-1 helicopter were established and were used to determine antenna system requirements.

Stub wing drawings and vibration data have not yet been received.

During the next report period it is planned that antenna feed designs and detailed analysis of the antenna system be initiated and the current efforts will continue.

Respectfully submitted,

R. D. Gober
Assistant Project Director

Approved:

D. G. Bodnar
Project Director
Project A-1551

A-1551

ENGINEERING EXPERIMENT STATION

GEORGIA INSTITUTE OF TECHNOLOGY • ATLANTA, GEORGIA 30332

10 October 1973

Commander, Frankford Arsenal
Attention: SMUFA-N6100
Philadelphia, PA 19137

Attention: N6100

Reference: Contract No. DAAA25-73-C-0648

Subject: Monthly Technical Status Report No. 3 for the period from 14 August to 13 September 1973

Gentlemen:

This status report covers the work performed on the referenced contract for the period from 14 August to 13 September.

Antenna system trade-off studies were initiated. Radar system requirements for the AH-1 helicopter as a radar system platform, antenna system packaging, environmental considerations and human factors are typical factors which will be considered. While these and other similar factors are far removed from antenna system hardware design, it is necessary that they be considered to establish performance requirements.

The present antenna system concept consists of two "nested" geodesic lens on one of the stub wings and a single geodesic lens on the other stub wing. The two nested geodesic lens will provide 60^{o} scan capability on its side of the AH-1 helicopter and the single geodesic lens will provide 60^{o} scan on the other side of the helicopter. In addition, it is intended that the two "nested" geodesic lens provide azimuth and elevation monopulse tracking on boresight.

The scan function will be accomplished by use of ring-switch feeds. Accurate aiming for weapons delivery will be accomplished by use of boresight-only monopulse feeds for the "nested" pair of geodesic lens.

During the next report period it is planned that current efforts continue with more emphasis being placed on hardware design.

Respectfully submitted,

R. D. Gober
Assistant Project Director

Approved:

D. G. Bodnar
Project Director
Project A-1551

A-1551

ENGINEERING EXPERIMENT STATION

GEORGIA INSTITUTE OF TECHNOLOGY • ATLANTA, GEORGIA 30332

14 December 1973

Commander, Frankford Arsenal
Attention: SMUFA-N6100
Philadelphia, PA 19137

Attention: N6100

Reference: Contract No. DAAA25-73-C-0648

Subject: Monthly Technical Status Report No. 4 for the period from 14 September to 13 October 1973

Gentlemen:

This status report covers the work performed on the referenced contract for the period 14 September to 13 October.

A. Antenna Requirements

During technical discussions early in the program with the Frankford Arsenal Technical Supervisor, Mr. Michael Milstead, a preliminary set of requirements was established for the leading-edge antenna. These requirements are listed in Table I. A beamwidth of 1^{o} or less is desired in azimuth and coverage of 15^{o} in elevation appears desirable. An azimuth scan sector of 120^{o} appears desirable and achievable. The frequency of operation will be established by Frankford Arsenal and will be either 35, 70, or 95 GHz.

B. Aperture Size

The aperture size in both the E- and H-planes is determined both by the available size for packaging the antenna and by the resolution requirements. The maximum size of the wing is roughly 10 inches high and 31 inches deep (front-to-back) as seen from Figure 1. However, the major portion of the wing is much smaller than this. The largest folded geodesic lens, non-gimbaled, which could be fitted into this envelope is about 15 to 25 inches in diameter.

An examination of beamwidth versus aperture size and frequency was made and is presented in Figure 2. A cosine shaped aperture distribution was assumed for simplicity. The cosine distribution raised to the first power produces -23dB sidelobes [1] while the cosine squared distribution produces -32 dB sidelobes. This range of sidelobe levels brackets those expected from the final antenna.

1. S. Silver, Microwave Antenna Theory and Design, McGraw-Hill, New York; 1948, pp 177-180

Table I

Baseline Antenna Parameters

Factor	Specification	
	Design Goal	Nominal
Az Coverage (Scan sector)	120^{o} total	———
El Coverage	———	$15\text{-}20^{o}$ total
Az BW	$\leq 1^{o}$	———
El BW	———	15^{o}
Power	———	20 kw
Bandwidth	———	1 or 2 GHz
Frequency	———	35, 70, or 95 GHz
Scan rate	———	6-10 per sec
Tracking Accuracy	1.2 mrad	———
Pulse Length	50 n sec	———
prf	———	4kHz
Dual Polarization	———	Desirable
Az Monopulse	Dead Ahead Only	———
El monopulse	Dead Ahead Only	———
Track While Scan	———	Desirable

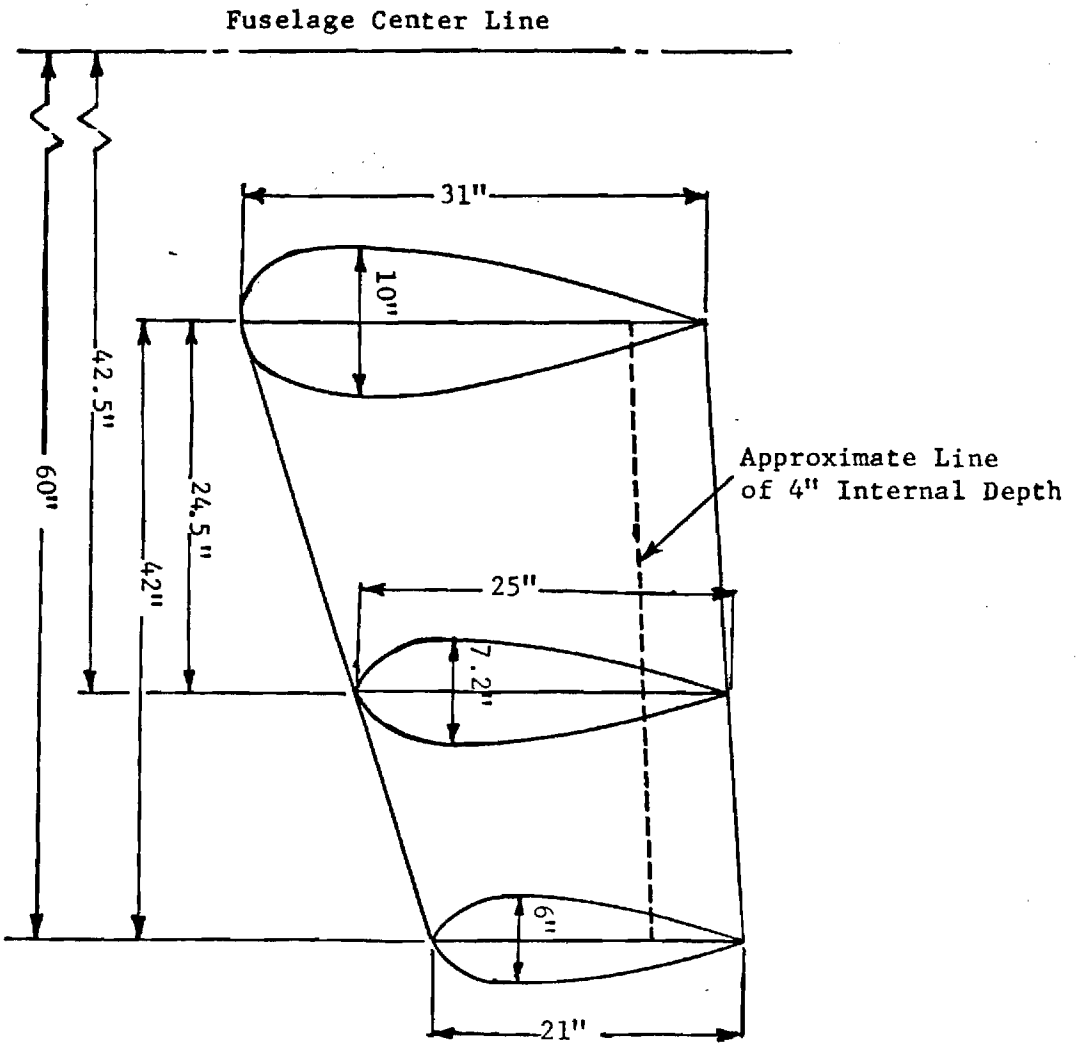

Figure 1. Approximate dimensions of AH-1G stub wing.

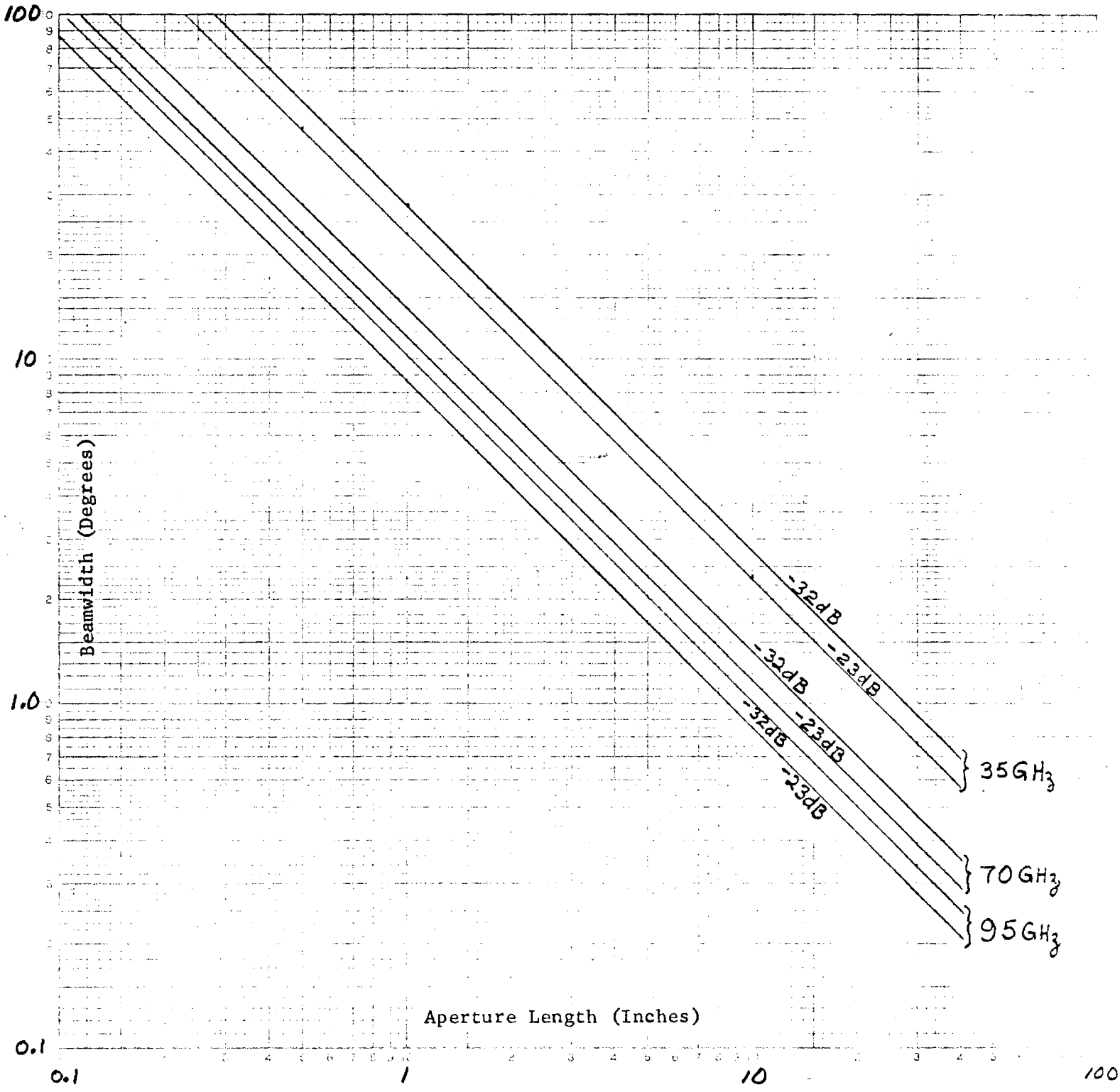

Figure 2. Beamwidth versus aperture length at millimeter frequencies for two different sidelobe levels.

From Figure 2 it can be seen that in order to achieve the desired 1^{o} beamwidth in azimuth an aperture of 25 inches is required at 35 GHz, 13 inches at 70 GHz and 9 inches at 95 GHz. To obtain the 15^{o} elevation beamwidth a 1.7 inch aperture is required at 35 GHz, an 0.85 inch aperture at 70 GHz and a 0.65 inch aperture at 95 GHz.

Respectfully submitted,

Donald G. Bodnar
Project Director
Project A-1551

DB/jb

A-1551

ENGINEERING EXPERIMENT STATION
GEORGIA INSTITUTE OF TECHNOLOGY • ATLANTA, GEORGIA 30332
17 December 1973

Commander, Frankford Arsenal
Attention: SMUFA-N6100
Philadelphia, PA 19137

Attention: N6100

Reference: Contract No. DAAA25-73-C-0648

Subject: Monthly Technical Status Report No. 5 for the period from 14 October to 13 November 1973

Gentlemen:

This status report covers the work performed on the referenced contract for the period from 14 October to 13 November.

A number of techniques are available to achieve the 1.2 mrad tracking accuracy desired by Frankford Arsenal for the leading-edge antenna. They include use of a large aperture, use of a lens in each wing as an interferometer pair, the use of a monopulse feed, and the use of a separate conical scan antenna.

A. Large Aperture Approach

If a large enough aperture is used then the desired azimuth resolution can be obtained from the antenna beam directly. A typical approximation is to use the 3dB beamwidth as the resolution capability of the beam. From an extrapolation of Figure 2 of status Report 4 it can be seen that an aperture length of 370, 190, and 135 inches is needed at 35, 70, and 95 GHz, respectively, in order to achieve a 1.2 mrad (0.069^{o}) beamwidth. Geodesic lenses in this size range obviously cannot be packaged in the stub wings. Hence, a technique other than the brute-force method of increasing the aperture size must be used to achieve the desired tracking accuracy.

An alternate approach is to use a lens in each wing as an interferometer pair. This approach is considered next.

B. Antenna Patterns Produced by Two Antennas Located in the Stub Wings

An analysis was made of the interferometer effects produced by two antennas (for example, geodesic lenses) located in the stub wings of the Cobra helicopter. The objective of the study was to determine how much, if any, azimuth beam sharpening could be obtained using the two antennas together. The antennas were modeled as two line sources each of length D and displaced by a distance L as shown in Figure 1. The total pattern will be represented by $E(\theta)$, the array factor by $AF(\theta)$, and the element pattern by $E_e(\theta)$. Thus

$$E(\theta) = E_e(\theta)\ AF(\theta) \tag{1}$$

Assume that Aperture 1 has a complex amplitude A_1 while Aperture 2 has a complex amplitude A_2. Then

$$AF(\theta) = A_1 e^{-jk \frac{L}{2} \sin \theta} + A_2 e^{+jk \frac{L}{2} \sin \theta}$$

Assume a symmetric phase difference of φ between the two elements, and that they have equal amplitudes, chosen to be 0.5 for convenience. Then

$$|A_1| = |A_2| = \frac{1}{2} \quad ,$$

$$\angle A_1 = -\frac{\varphi}{2} \quad , \text{ and}$$

$$\angle A_2 = +\frac{\varphi}{2} \quad .$$

Thus

$$AF(\theta) = \frac{1}{2} e^{-j(k \frac{L}{2} \sin \theta + \frac{\varphi}{2})} + \frac{1}{2} e^{j(k \frac{L}{2} \sin \theta + \frac{\varphi}{2})} \quad ,$$

or

$$AF(\theta) = \cos \Psi \ . \tag{2}$$

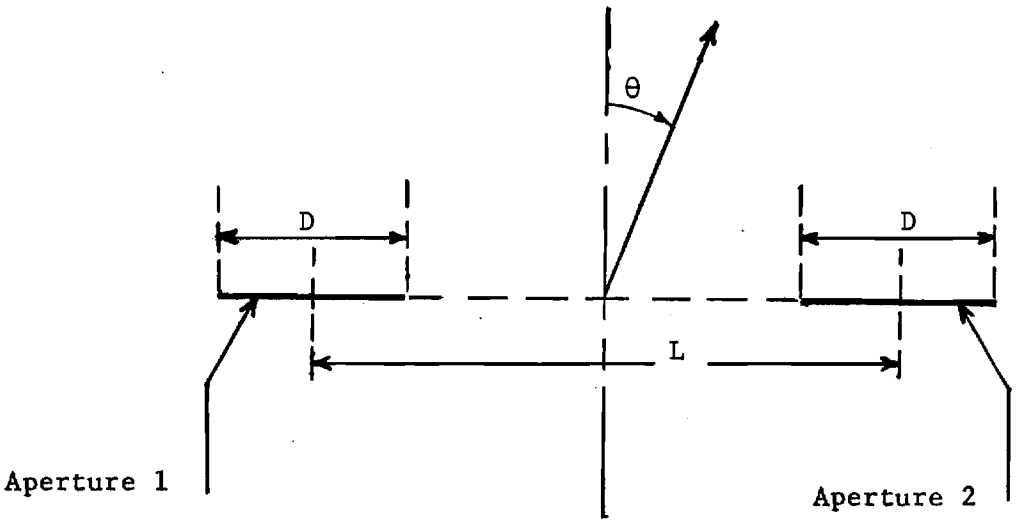

Figure 1. Two displaced, identical antennas.

where

$$\Psi = k\frac{L}{2}\sin\theta + \frac{\varphi}{2} = \pi\left(\frac{L}{\lambda}\right)\sin\theta + \frac{\varphi}{2} \ . \qquad (3)$$

For ease of computation a simple far field pattern was assumed for geodesic lens, namely

$$E_e(\theta) = \left[\frac{\sin\left(\frac{u}{n}\right)}{\left(\frac{u}{n}\right)}\right]^n \qquad (4)$$

where $n = 1, 2, 3, \cdots$ and $u = \pi\,(D/\lambda)\sin\theta$. For $n = 1$ the pattern (4) is produced by a uniformly illuminated line source for which the sidelobe level is -13.2dB, and the beamwidth is $50.8^{\circ}\ D/\lambda$. For $n = 2$ the pattern (4) is produced by a triangular distribution on the line source for which the sidelobe level is -26.4dB and beamwidth is $73.4^{\circ}\ D/\lambda$.

Patterns were calculated for the following set of parameters:

Lens diameter	D = 25"
Lens spacing	L = 40", 60", 80"
Wavelength	λ = 0.347" (35 GHz), 0.169" (70 GHz)
Phase difference	$\varphi = 0^{\circ}$
Aperture taper	n = 2 (triangular)

These six patterns are shown in Figures 2-7. A triangular aperture distribution was chosen since it gave reasonable, ie -26.4dB, sidelobes. Note from the figures that the array factor samples the element pattern as expected. Note also that the first interferometer lobe is very high, and is independent of frequency. The level of the first interferometer lobe is tabulated in Table II.

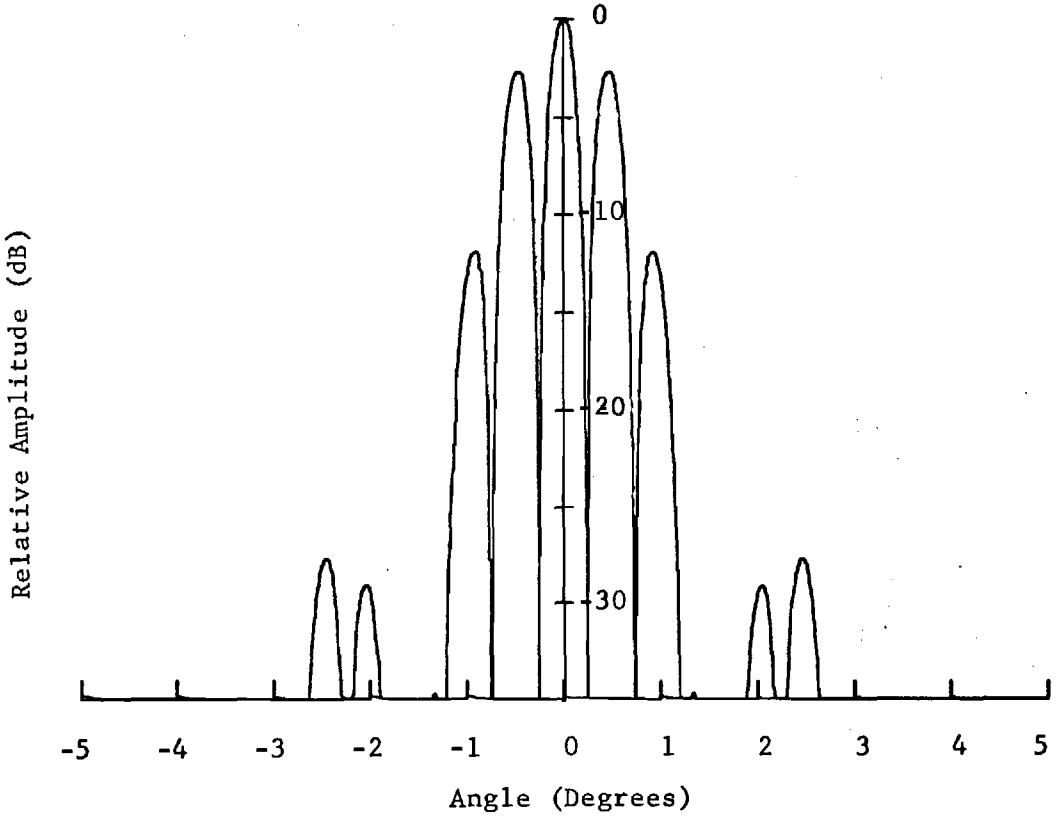

Figure 2. Pattern produced by two line source antennas with D = 25 inches, L = 40 inches, n = 2, and f = 35 GHz.

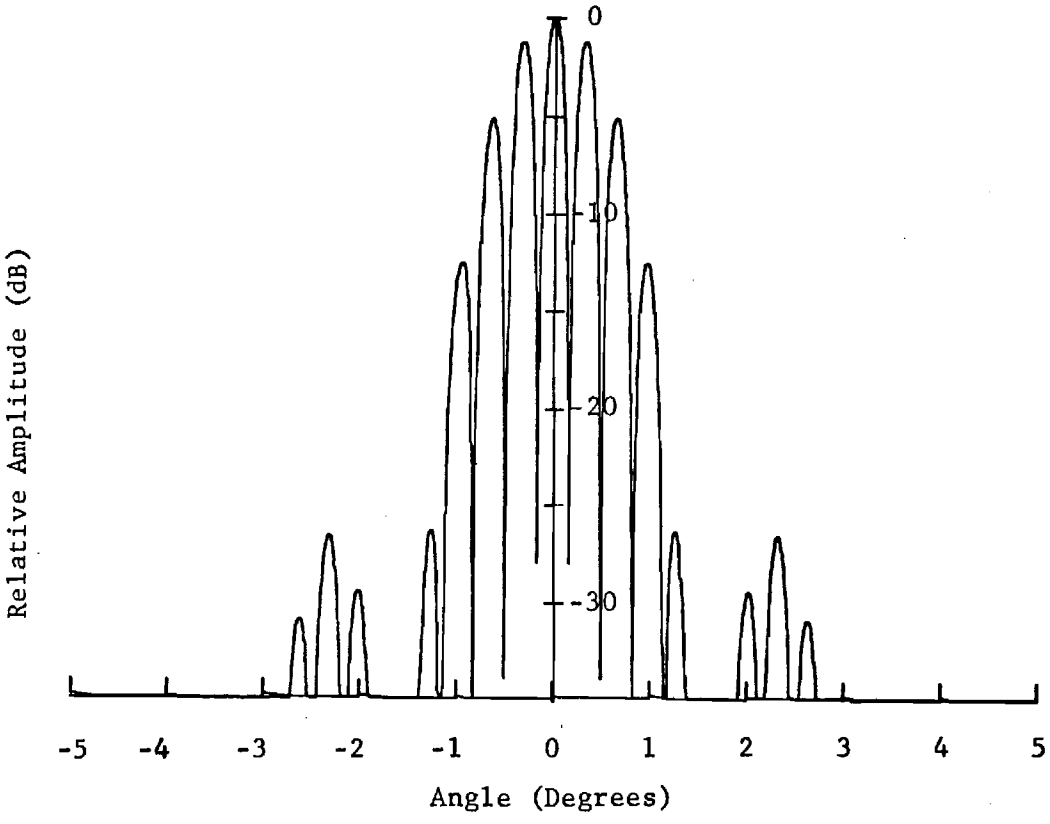

Figure 3. Pattern produced by two line source antennas with D = 25 inches, L = 60 inches, n = 2, and f = 35 GHz.

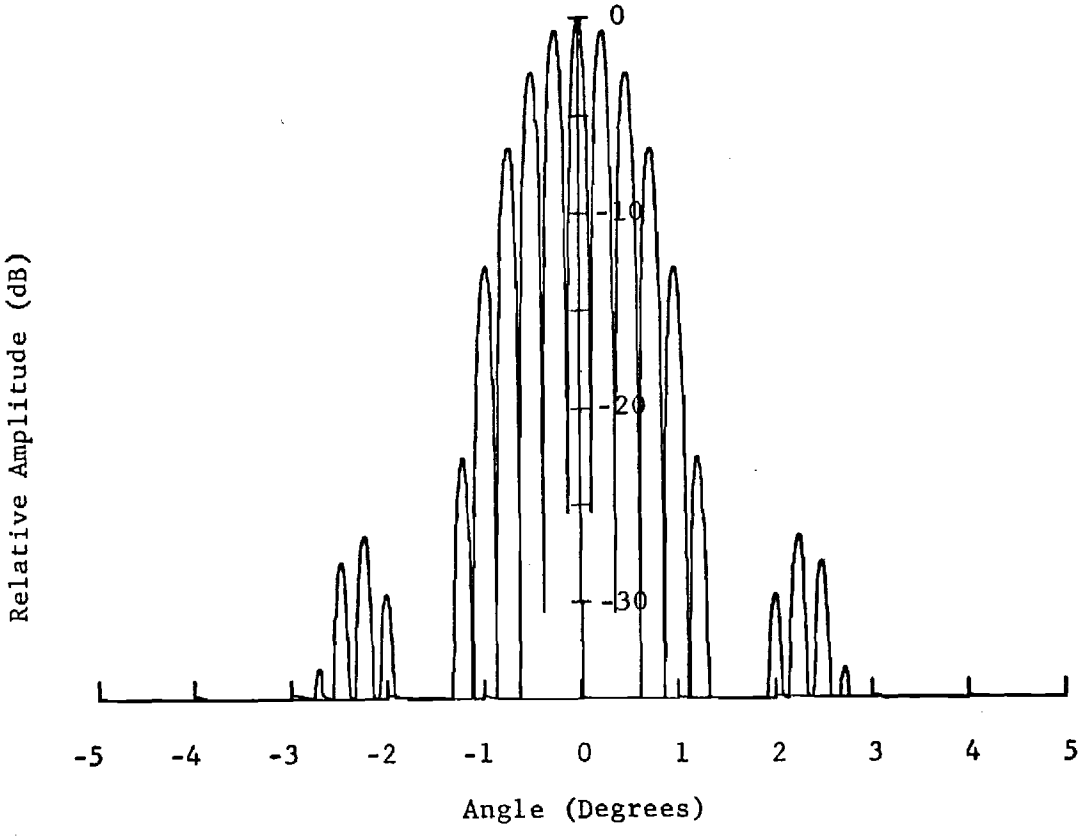

Figure 4. Pattern produced by two line source antennas with D = 25 inches, L = 80 inches, n = 2, and f = 35 GHz.

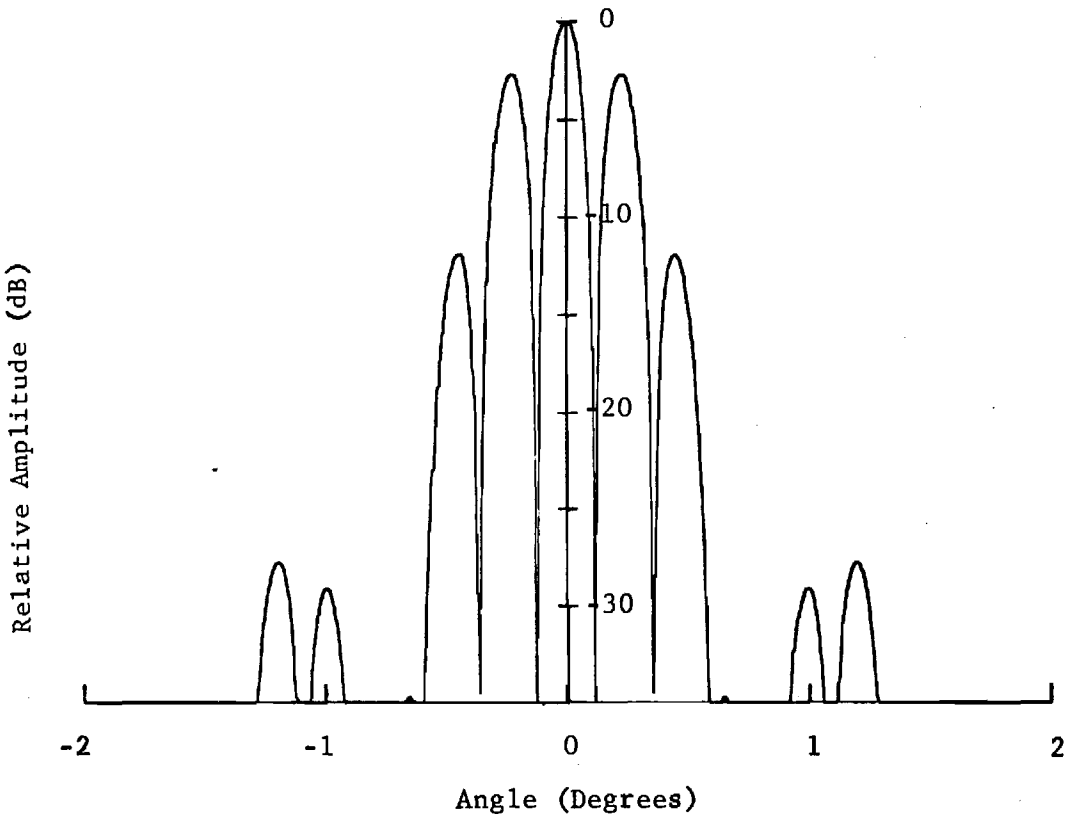

Figure 5. Pattern produced by two line source antennas with D = 25 inches, L = 40 inches, n = 2, and f = 70 GHz.

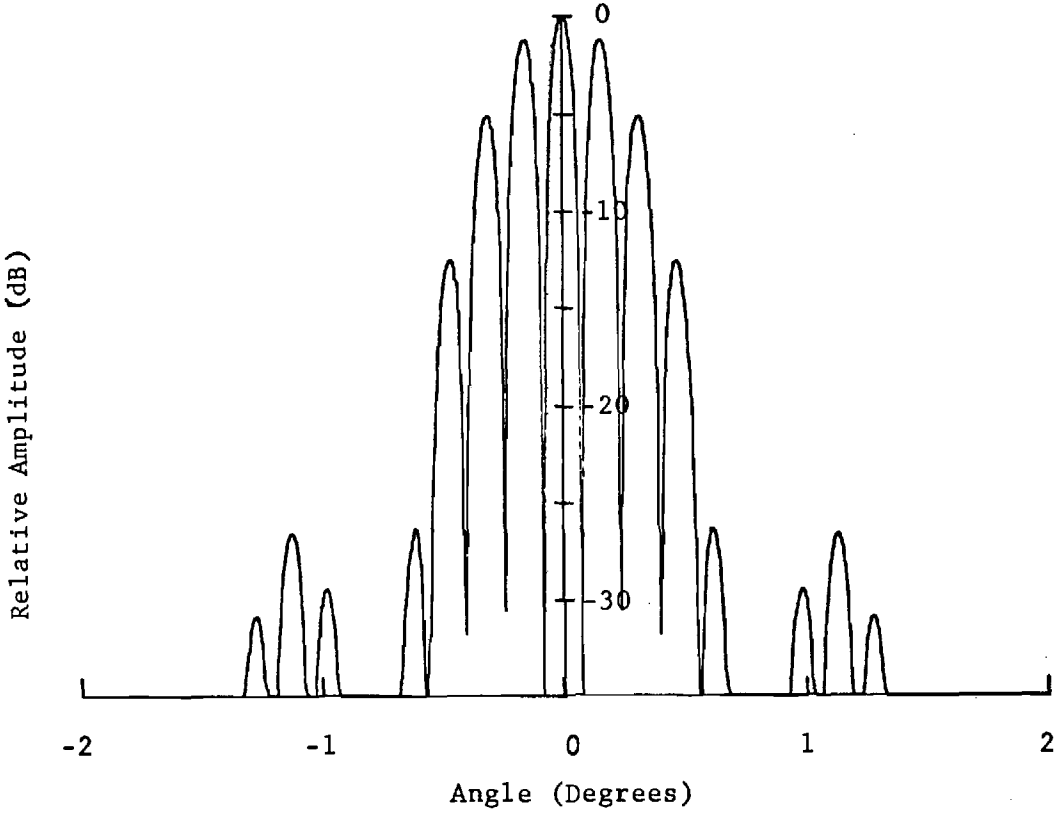

Figure 6. Pattern produced by two line source antennas with D = 25 inches, L = 60 inches, n = 2, and f = 70 GHz.

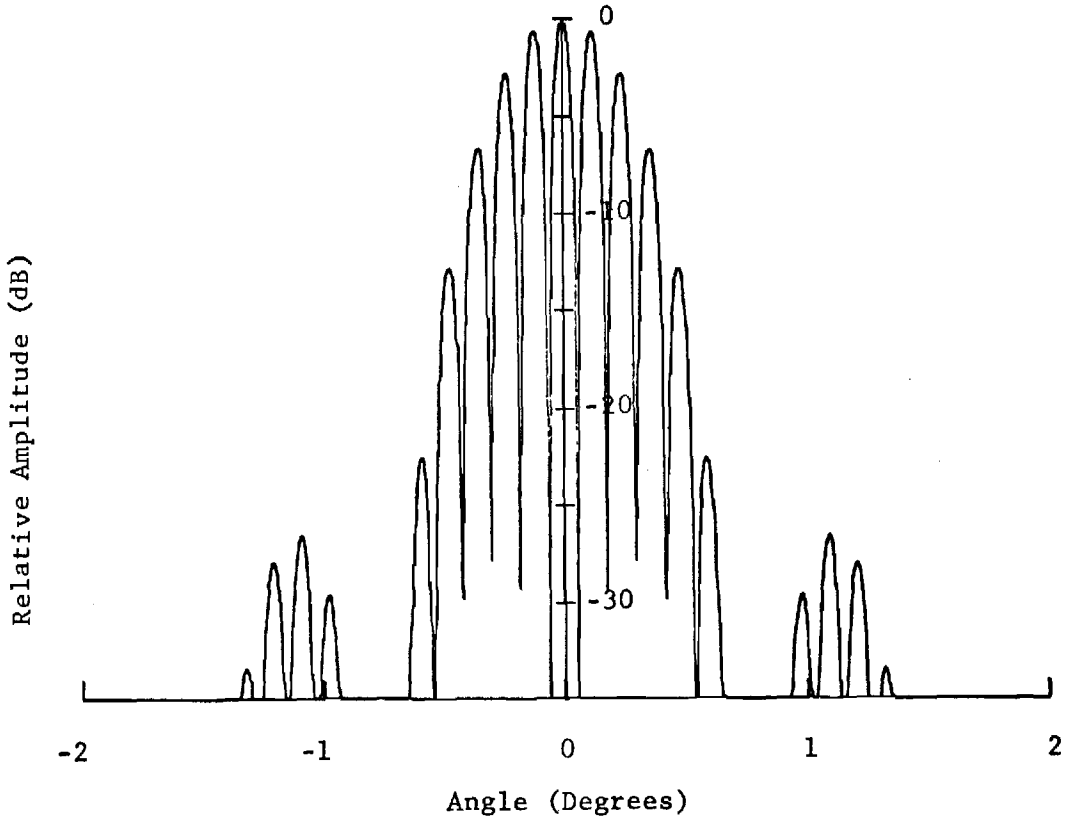

Figure 7. Pattern produced by two line source antennas with D = 25 inches, L = 80 inches, n = 2, and f = 70 GHz.

Table II

Interferometer Lobe Level Versus Separation

L	First Interferometer Lobe Level (n=2)
40"	-2.7dB
60"	-1.2dB
80"	-0.7dB

The lens must be separated about 70 to 80 inches since the Cobra body is 36 inches wide at the wings and the lenses are 25 inches in diameter. Thus although the mainbeam of the pattern has been narrowed by using the two antennas as an interferometer, the amplitude of adjacent interferometer lobes are so close to that of the main beam (only about 1dB down) that it would be impossible to distinguish which lobe the target was on in a tactical situation.

The level of the interferometer lobes can be reduced by decreasing the taper on the aperture since this narrows the main beam. The sidelobe level of the element pattern is increased, however, by doing this. Figures 8-10 show the patterns produced for a uniformly illuminated (n = 1) aperture at 35 GHz. For a 70 inch lens spacing the interferometer lobes are only 2dB below the main beam. As seen from Figures 2-7 the interferometer lobe levels are independent of frequency. Hence, the interferometer lobes are unacceptably high even with a uniformly illuminated aperture.

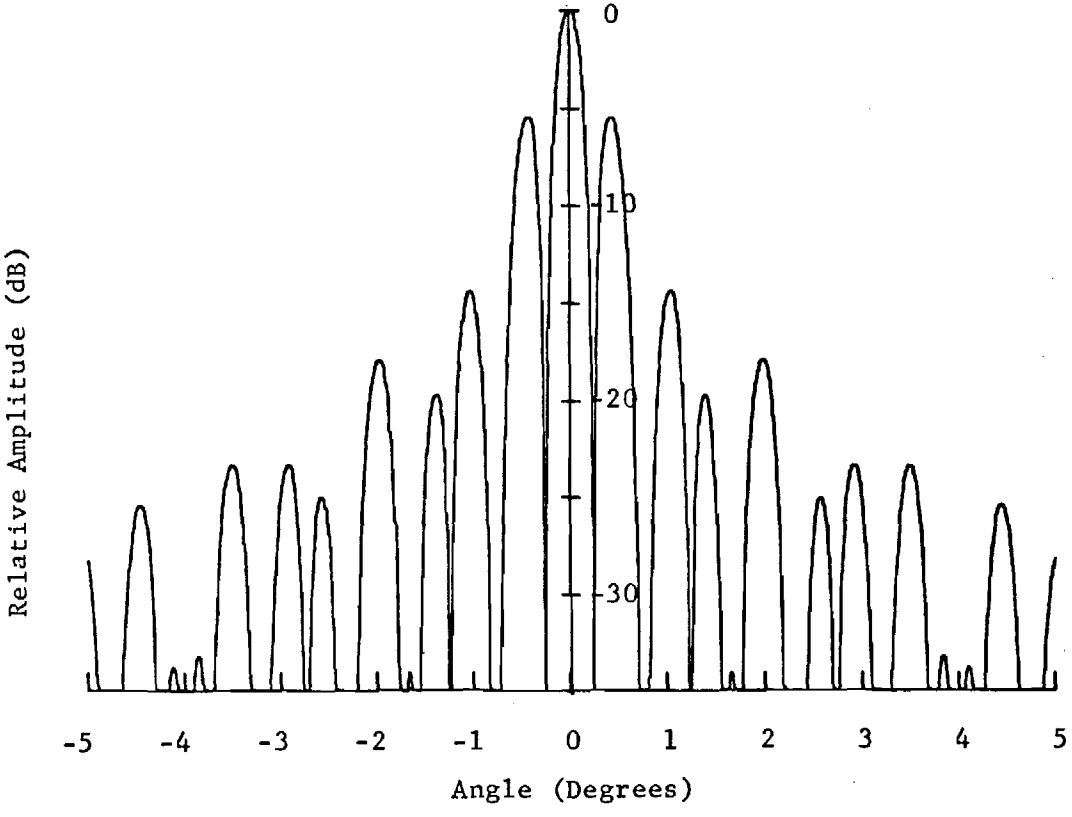

Figure 8. Pattern produced by two line source antennas with D = 25 inches, L = 40 inches, n = 1, and f = 35 GHz.

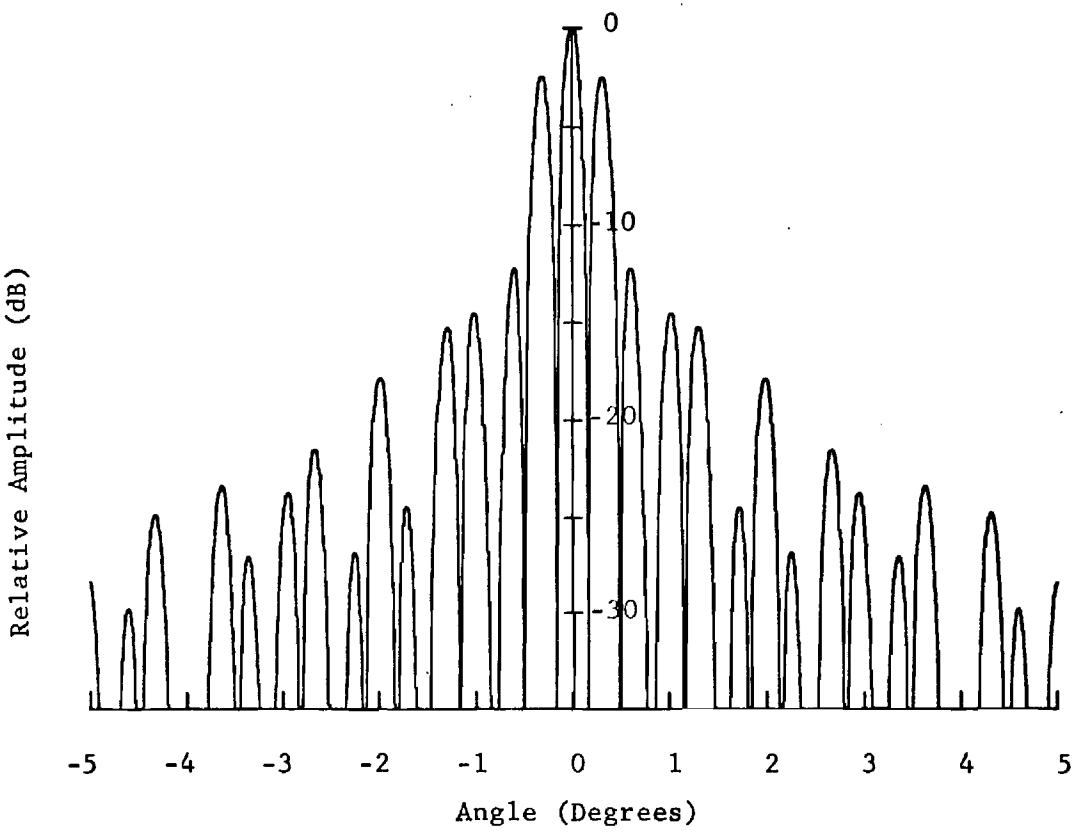

Figure 9. Pattern produced by two line source antennas with D = 25 inches, L = 60 inches, n = 1, and f = 35 GHz.

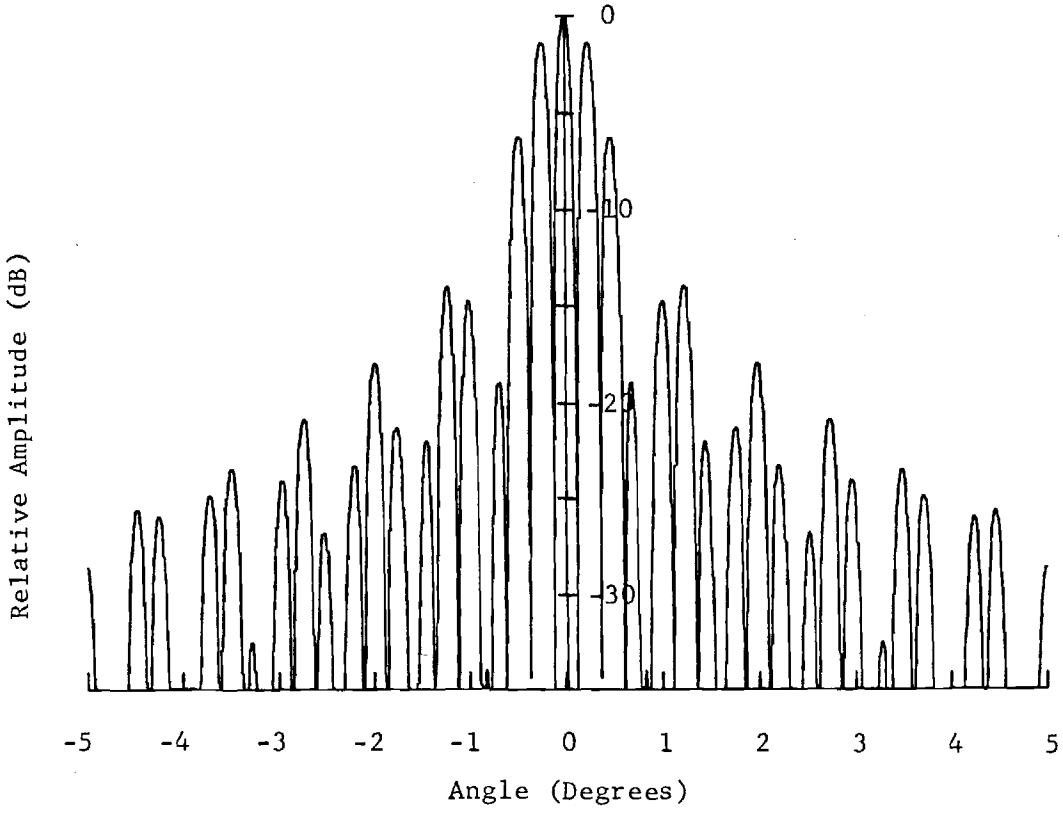

Figure 10. Pattern produced by two line source antennas with D = 25 inches, L = 80 inches, n = 1, and f = 35 GHz.

From the preceeding analysis it is concluded that use of a lens in each wing as an interferometer pair will not perform satisfactorily for the leading-edge geometry.

C. Alternate Approaches

It is anticipated that both monopulse and conical scan techniques can provide the desired tracking accuracy. These techniques will be investigated during the next reporting period.

Respectfully submitted,

Donald G. Bodnar
Project Director
Project A-1551

A-1551

ENGINEERING EXPERIMENT STATION
GEORGIA INSTITUTE OF TECHNOLOGY • ATLANTA, GEORGIA 30332

20 December 1973

Commander, Frankford Arsenal
Attention: SMUFA-N6100
Philadelphia, PA 19137

Attention: N6100

Reference: Contract No. DAAA25-73-C-0648

Subject: Monthly Technical Status Report No. 6 for the period from 14 November to 13 December 1973

Gentlemen:

This status report covers the work performed on the referenced contract for the period from 14 November to 13 December.

As mentioned in Status Report No. 5, two possible ways of achieving the desired tracking accuracy are through the use of monopulse or conical scanning. These two approaches have been examined and are discussed below. A few comments about geodesic Luneberg lenses are required before proceeding.

A. Geodesic Luneberg Lenses

The basic type of antenna considered is a geodesic Luneberg lens. The geodesic Luneberg lens is a waveguide analog of a plane slice through a three-dimensional Luneberg lens [1]. The geodesic Luneberg lens has the property that a point-source feed on its periphery is transformed into a line source diametrically opposite the feed point. Thus the geodesic lens provides collimation of energy in one plane. Collimation of energy in the other plane can be obtained, for example, through the use of a parabolic cylinder fed by the line source output of the geodesic lens. Geodesic lenses are excellent scanning antennas even at millimeter wavelengths. Geodesic lenses have been built at Georgia Tech from X-band and V-band (70 GHz) [2, 3, 4]. They are very broadband devices that typically operate over an entire waveguide band. Thus they are compatible with doppler signal processing and frequency agile transmitters.

1. Johnson, R. C., "The Geodesic Luneberg Lens," Microwave Journal, August 1962, pp 76-85.
2. Johnson, R. C., "Radiation Patterns from a Geodesic Luneberg Lens," Microwave Journal, July 1963, pp 68-70.
3. Alford, S. T. et al, "Microwave Scanning Antenna Studies in Support of Advanced Echo Range Requirements (U)," Final Engineering Report, Prime Contract N00017-62-C-0604, subcontract APL/JHU 271845, Georgia Institute of Technology, June 1973.
4. Long, M. W. and Allen, G. E., Jr., "Combat Surveillance Radar," Final Report on Contract DA 36-039 SC-74870, Georgia Institute of Technology AD 318212, June 1960.

B. Monopulse and Conical Scan

Two plane monopulse tracking was examined for the leading-edge antenna. The concept was to provide a dual mode feed for the geodesic lens for azimuth monopulse and to stack two lenses one above the other to provide elevation plane monopulse. The antenna concept is capable of providing dual plane monopulse. However, an examination of the receiver requirements precludes the use of monopulse at this time. The phase difference between receiver channels must be maintained to within 25^{0} or better for reasonably proper performance according to Page [5]. It appears that off-the-shelf receiver components at 95 GHz cannot currently provide such phase stability and so monopulse must be ruled out at this time. As component technology improves, it may be possible to use monopulse at 95 GHz at a later time. However, the system complexity will still be present since three receivers will be required.

Conical scanning on the other hand can be implemented with off the shelf receiver components. In addition, its receiver circuitry is considerably simpler than that in monopulse. In many instances the tracking performance of conical scan is as good as that of monopulse. Hence it appears that conical scan is the preferred tracking technique at the present time (and possibly in the future too).

A no-cost time extension to the contract was requested during this reporting period. The additional time is needed to evaluate technical manuals and data from the Army.

As of December 1, 1973 a total of $17,831.33 had been spent on the project or 45% of the total contract value. The expenditure rate was lower than anticipated since the total planned complement of personnel could not be assigned to the effort due to the fact that data on the AH-1G arrived late at Georgia Tech. The requested time extension should permit the previously planned tasked to be completed.

Respectfully submitted,

Donald G. Bodnar
Project Director
Project A-1551

DB/jb

---

5. R. M. Page, "Monopulse Radar," IRE National Convention Record, Vol. 3 Pt. 8, pp 132-134, 1955.

A-1551

ENGINEERING EXPERIMENT STATION

GEORGIA INSTITUTE OF TECHNOLOGY • ATLANTA, GEORGIA 30332

23 January 1974

Commander, Frankford Arsenal
Attention: SMUFA-N6100
Philadelphia, PA 19137

Attention: N6100

Reference: Contract No. DAAA25-73-C-0648

Subject: Monthly Technical Status Report No. 7 for the period from 14 December 1973 to 13 January 1974

Gentlemen:

This status report covers the work performed on the referenced contract for the period 14 December 1973 to 13 January 1974.

The results of the analysis to date indicate that the optimum antenna geometry for the 95 GHz modified stub wing installation consists of three antennas. One geodesic lens will be placed in each wing as shown in Figure 1. Each lens provides 60^{o} of search coverage from dead ahead for a total of 120^{o} search coverage for the antenna system. Data from the two antennas will be combined for presentation on a single display. This will allow the operator to designate (sequentially) targets of interest with a single curser system. The conical scan tracking antenna will then be automatically positioned on the designated target and commence automatic tracking independent of helicopter motion. Doppler signature data will be extracted from the track signal to aid in target identification. The tracking information will also be used to que others sensors and/or weapons delivery.

The plan view shown in Figure 1 depicts two possible geodesic lens locations. The lower installation depicts the lens attached in front of the present stub wing of the AH-1G. The upper installation depicts a lens built inside of the present wing. The size of the wing was increased for both installations in order to maintain the same lift to drag ratio as exists in the present wing. The size of the wing is roughly the same for either installation. It should be noted that the stub wings of the Cobra are not aerodynamic lifting surfaces but merely weapon store racks.

The lenses will most likely be gimbaled to remove most of the aircraft motion. Figure 2 shows the wing size for $\pm 15^{o}$ stabilization in both pitch and roll. The height of the wing can be reduced by decreasing the roll stabilization

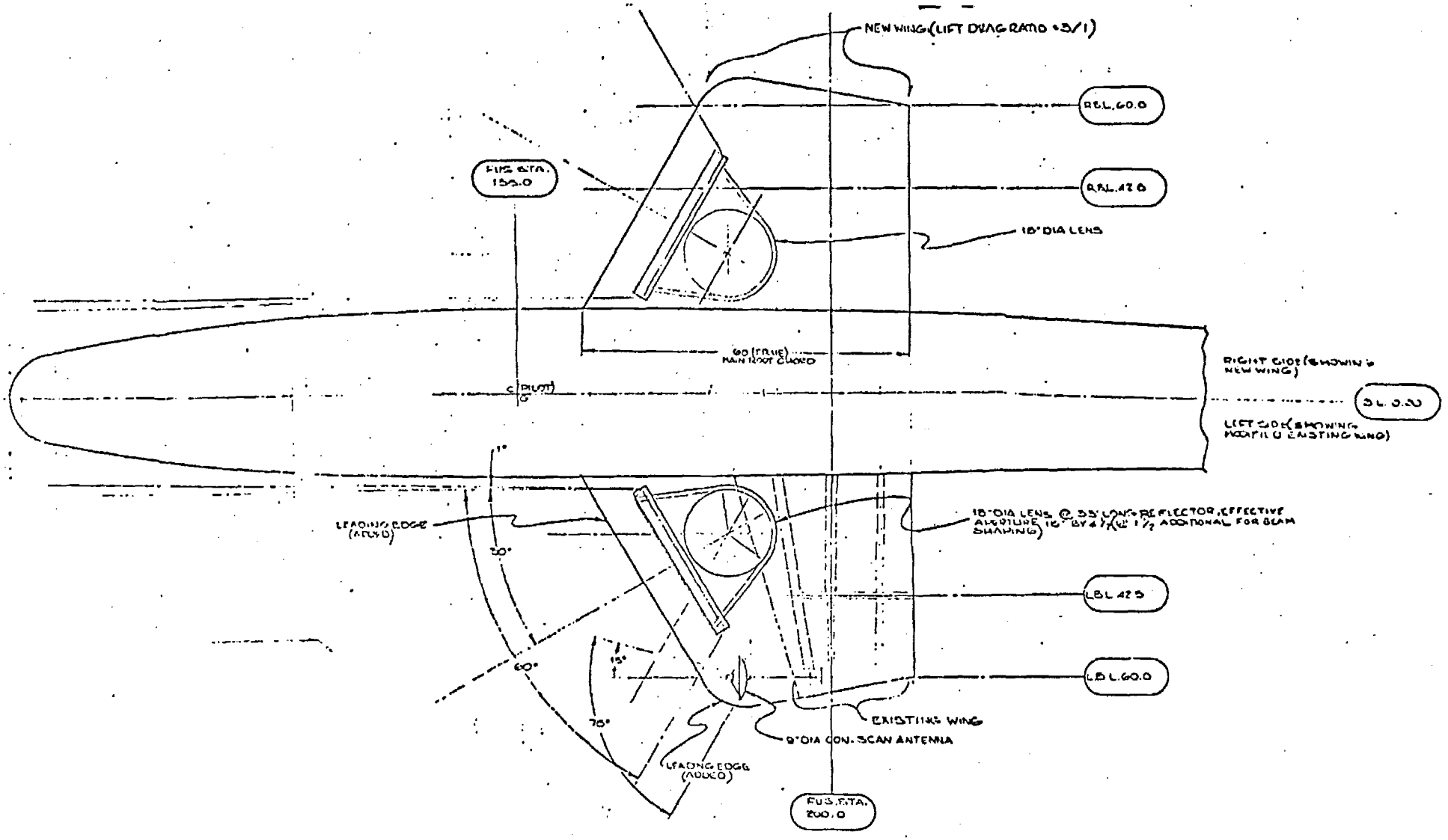

Figure 1 Plan view of stub wing antenna installation.

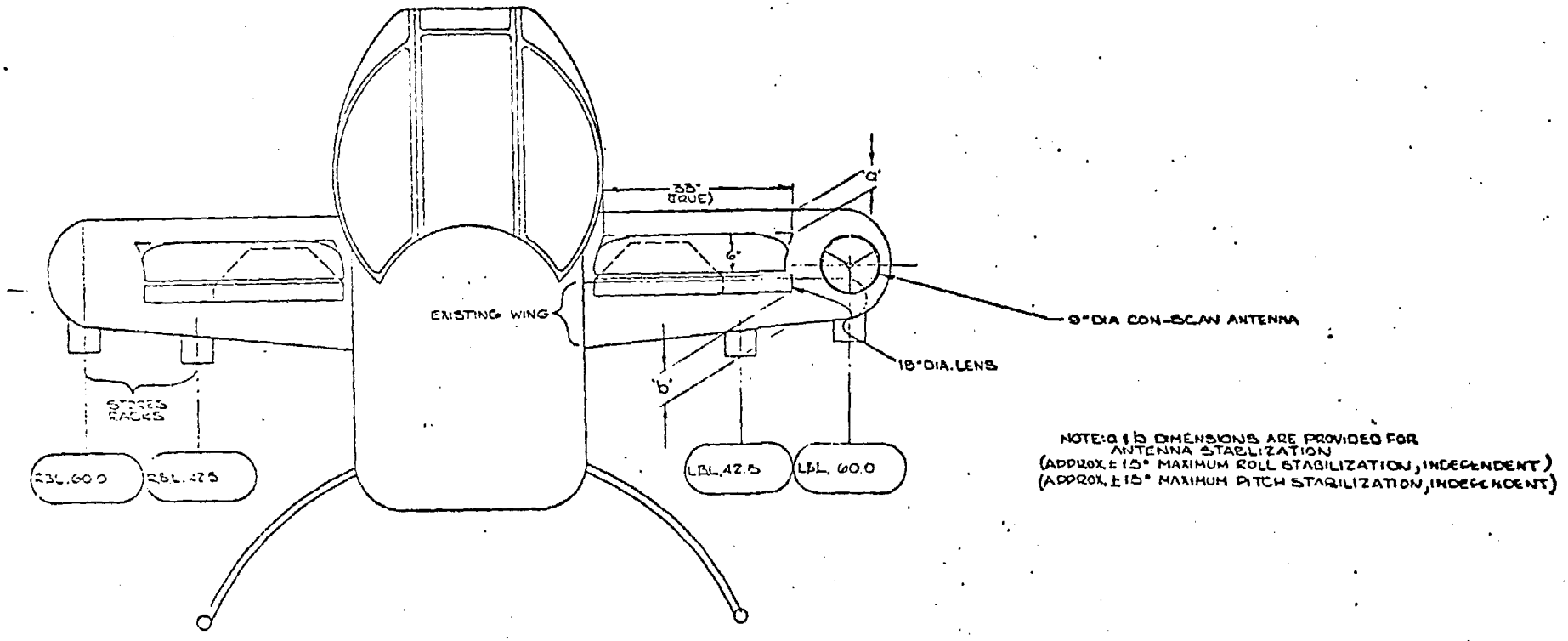

VIEW LOOKING AFT

Figure 2. Front view of stub wing antenna installation.

requirements. The wing appears fatter in Figure 2 than it actually is since it is a front view with the aircraft horizontal. The wings are tilted with respect to horizontal and so appear larger in this frontal projection.

Respectfully submitted,

Donald G. Bodnar
Project Director
Project A-1551

DB/jb

A-1551

ENGINEERING EXPERIMENT STATION

GEORGIA INSTITUTE OF TECHNOLOGY • ATLANTA, GEORGIA 30332

21 March 1974

Commander, Frankford Arsenal
Attention: SMUFA-N6100
Philadelphia, PA 19137

Attention: N6100

Reference: Contract No. DAAA25073-C-0648

Subject: Monthly Technical Status Report No. 8 for the period from 14 January to 14 February 1974

Gentlemen:

This status report covers the work performed on the referenced contract for the period from 14 January to 14 February 1974.

Two plane monopulse tracking was examined for the leading-edge antenna. The concept was to provide a dual mode feed for the geodesic lens for azimuth monopulse and to stack two lenses one above the other to provide elevation plane monopulse. The antenna concept is capable of providing dual plane monopulse. However, an examination of the receiver requirements precludes the use of monopulse at this time. The phase difference between receiver channels must be maintained to within 25^{o} or better for reasonably proper performance according to Page.[1] It appears that off-the-shelf receiver components at 95 GHz cannot currently provide such phase stability and so monopulse must be ruled out at this time. As component technology improves, it may be possible to use monopulse at 95 GHz at a later time. However, the system complexity will still be present since three receivers will be required.

Conical scanning, on the other hand, can be implemented with off-the-shelf receiver components. In addition, its receiver circuitry is considerably simpler than that in monopulse. In many instances the tracking performance of conical scan is as good as that of monopulse. Hence it appears that conical scan is the preferred tracking technique at the present time (and possibly in the future too).

A time and cost estimate to build the recommended antenna system is being prepared.

Respectfully submitted,

D. G. Bodnar
Project Director

[1] R. M. Page, "Monopulse Radar," IRE National Convention Record Vol. 3, Pt. 8, pp 132-134, 1955.

File : A-1551

EXPERIMENT STATION 225 North Avenue, Northwest Atlanta, Georgia 30332

22 March 1974

Commander, Frankford Arsenal
Attention: SMUFA-N6100
Philadelphia, PA 19137

Attention: N6100

Reference: Contract No. DAAA25-73-C-0648

Subject: Monthly Technical Status Report No. 9 for the period from 14 February to 14 March 1974

Gentlemen:

This status report covers the work performed on the referenced contract for the period from 14 February to 14 March 1974.

The final report on the leading-edge study is being prepared. A draft of the report was reviewed by Mr. Michael Milsted during his visit to Georgia Tech on March 13, 1974.

A time and cost estimate has been made to perform a detailed design to build and to test the two geodesic lenses and the conical scanned Cassegrain antenna that will be reported in the final report on the above referenced contract. It is estimated that if constructed at the Georgia Institute of Technology, a period of approximately fourteen (14) months would be required after initiation of contract to complete the work and that the cost would be approximately $300,000. A detailed cost and time estimate will be provided to Frankford Arsenal in a forthcoming proposal.

A number of subsystems must be built and certain tasks accomplished before the leading-edge radar is operational. These include the following:

1. Antenna System
2. Gimbals for Antennas
3. New Wing
4. Radome
5. Integrated System Configuration Study
6. Hardware Feasibility Demonstration Radar
7. Brassboard/Prototype Development Radar

The above time and cost estimate is for accomplishing number 1. of the above list. We would, of course, be interested in assisting Frankford Arsenal in completing any or all of the remaining tasks.

Respectfully submitted,

D. G. Bodnar
Project Director

AN ANTENNA AND RADOME FOR A 95 GHz ARTIC SURFACE EFFECT VEHICLE RADAR*

by

D. G. Bodnar
Systems and Techniques Department
Engineering Experiment Station
Georgia Institute of Technology
Atlanta, Georgia 30332

and
C. C. Kilgus
Space Systems Division
Applied Physics Laboratory
Johns Hopkins University
8621 Georgia Avenue
Silver Spring, Maryland 20910

I. INTRODUCTION

An antenna and a radome have been developed at 95 GHz for use in evaluating certain terrain-avoidance radar techniques that are contemplated for an artic surface-effect vehicle (SEV) radar. The antenna and radome are both physically and electrically large yet they maintain their performance over a wide range of environmental conditions. The pillbox antenna produces a $0.1^{\circ} \times 1.5^{\circ}$ fan beam with 51 dB of gain. An unusual feature of the antenna is that its beam is focused in the Fresnel zone to improve short-range resolution. The 13.4 foot diameter metal space frame radome introduces less than 1 dB insertion loss and no detectable boresight shift.

II. ANTENNA CHARACTERISTICS

The terrain-avoidance techniques planned for the Applied Physics Laboratory 95 GHz SEV radar require a $0.1^{\circ} \times 1.5^{\circ}$ fan beam antenna. This beam can conceptually be produced by a number of simple antenna geometries such as a pillbox, a hog horn feeding a parabolic cylinder, or a dielectric lens corrected horn. Since the antenna will be subjected to

*This work was supported under Contract N00017-72-C-4401 (subcontract APL/JHU 372113).

vibration and quite probably thermal stress, it is necessary that the structure be stiff in order to maintain the requisit shape and alignment. The pillbox geometry was selected because (1) the reflector shape could be more easily maintined, (2) the primary feed could be aligned easily, and (3) the focal point and reflector shape tend to be self compensating with temperature if the same metal is used throughout the structure.

A conceptual drawing of the pillbox that was fabricated is shown in Figure 1. A primary feed horn having a 0.165 inch H-plane by 0.245 inch E-plane aperture is placed near the focal point of a 35 inch focal length, 100 inch long parabolic reflector. The parallel plates are 1/3-inch thick pure aluminum (Alclad) with the polished surface on the active side. The parallel plates are spaced 2λ = 0.250 inch apart to reduce I^2R loss. No moding problems were encountered with the oversized spacing. The parallel plates were tapered down to 0.050-inch spacing in the cylindrical bend region and then flared to a line-source feed with a 0.280 inch E-plane by 100 inch H-plane aperture. A 0.005-inch thick Mylar radome covers this line source horn. The line source feed illuminates a 5.8 inch high by 100 inch long parabolic cylinder reflector. The primary feed is moved away from the parabolic reflector by approximately 0.030 inch in order to focus the beam at 4400 feet and thus improve short range resolution.

The antenna pattern was measured at 1000 feet, 4400 feet and 2 1/8 miles ($2D^2/\lambda$ = 2.5 miles) and over a -20°F to $+80^{\circ}$F temperature range. A tabulation of measured performance is given in Tables I through IV. Calculated I^2R loss in the paralled plates is 0.9 dB. Measured VSWR is less than 1.3:1 over 93.5 to 96.0 GHz. A typical H-plane pattern is shown in Figure 2. Beyond about $\pm 10^{\circ}$ from the main beam the H-plane sidelobes were at least -40 dB.

III. RADOME CHARACTERISTICS

The 95 GHz antenna is protected from the hostile artic environment by a 13.4 foot diameter radome developed by ESSCO Corp., Concord, Mass. The radome is a metal space frame design, i.e. it consists of webbs of pseudorandomly placed metal members holding triangular shaped dielectric membranes. The membrane material is ESSCOLAM V, a strong

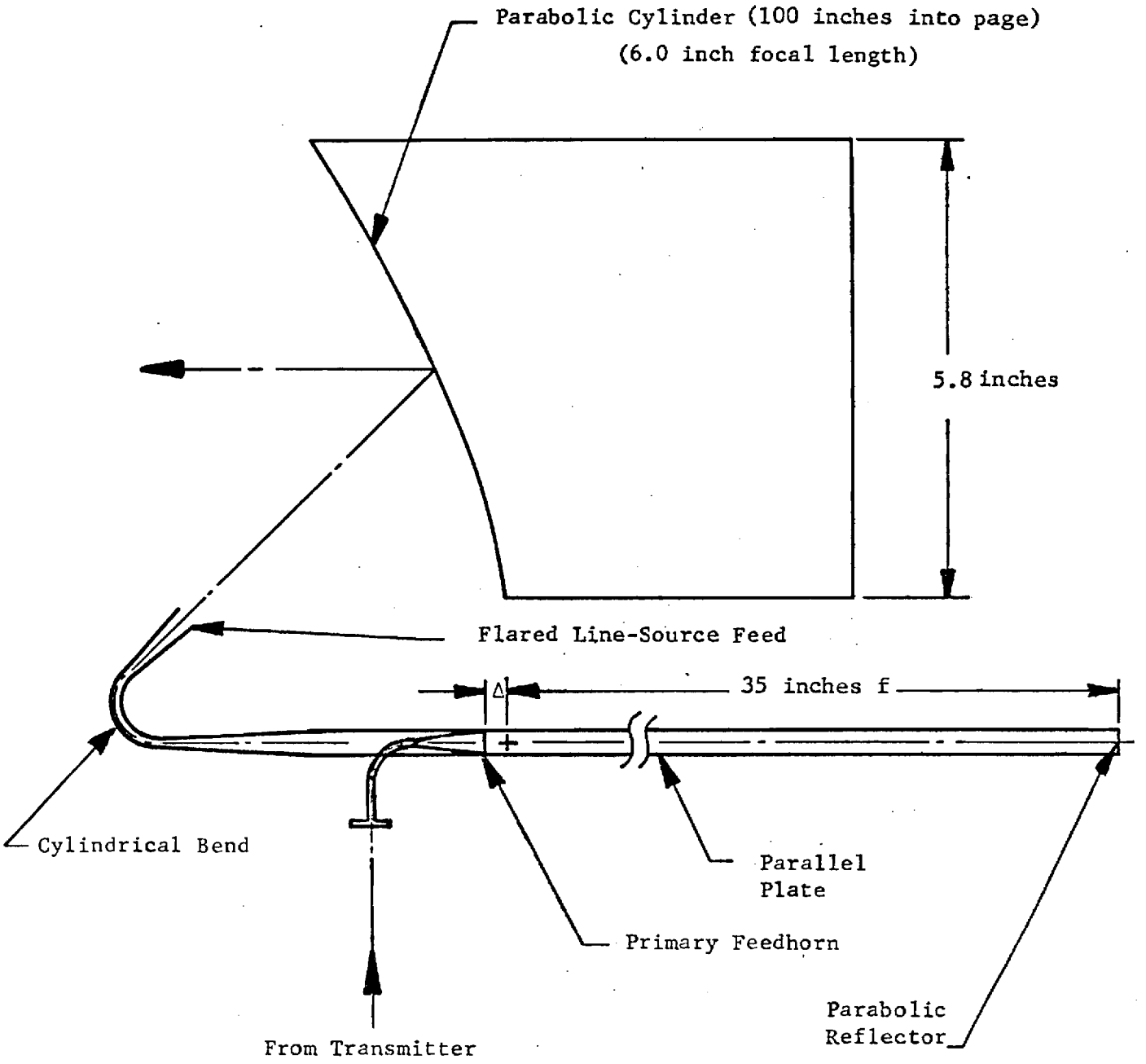

Figure 1. Antenna configuration consisting of primary feed, pillbox, line-source feed, and parabolic cylinder.

TABLE I

Gain, beamwidth, and sidelobes at 50°F and at a range of 2-1/8 miles.

Freq. (GHz)	Gain (dB)	Beamwidth		Sidelobe Level (dB)	
		H-Plane	E-Plane	H-Plane	E-Plane
95.0	48.9	0.11°	1.49°	-28.2	-22.0

TABLE II

Gain, beamwidth, and sidelobes at 55°F and at a range of 1000 feet.

Freq. (GHz)	Gain (dB)	Beamwidth		Sidelobe Level (dB)	
		H-Plane	E-Plane	H-Plane	E-Plane
95.0	47.6	0.15°	1.45	-27.0	-21.0

TABLE III

Gain, beamwidth, and sidelobes averaged over frequency at a range of 4400 feet.

Temp. (°F)	Measured Gain (dB)	Corrected Gain* (dB)	Beamwidth		Sidelobe Level (dB)	
			H-Plane	E-Plane	H-Plane	E-Plane
-20	49.8	51.8	0.11°	1.47°	-26.2	-20.3
0	50.4	51.6	0.11°	1.47°	-26.1	-20.7
+70	51.3	51.3	0.11°	1.47°	-27.0	-20.7

TABLE IV

Gain, beamwidth, and sidelobes averaged over temperature and frequency at a range of 4400 feet.

Measured Gain (dB)	Corrected Gain (dB)	Beamwidth		Sidelobe Level (dB)	
		H-Plane	E-Plane	H-Plane	E-Plane
50.5	51.6	0.11°	1.47°	-26.4	-20.5

*Gains measured with heavy frost on both the line-source radome and on the parabolic-cylinder reflector have had 2dB added to them.

dielectric with a dielectric constant of 2.8 and a loss tangent of 0.012 (at 95 GHz). The material thickness is $\lambda/2$ at 95 GHz. The membrane surface is coated with TEDLAR to prevent water adherance. The metal members are rectangular in cross section with dimension 0.35 inches x 1.15 inches with the long dimension toward the antenna. The longest member is 33.6 inches in length. The radome is designed to operate in 150 mph wind and over a temperature range of $-65^{o}F$ to $+140^{o}F$. It will withstand an ice and snow load of 75 psf. A blower system prevents the formation of ice on the radome surface by circulating air within the radome surface.

An extensive series of tests were conducted on the antenna/radome combination. It was determined that the radome insertion loss was less than 1 dB as had been theoretically predicted. No boresight shift was detected indicating it was certainly less than 0.1 beamwidths, i.e. $< 0.01^{o}$. Changes in levels of 20 dB sidelobes were less than 1 dB, 25 dB sidelobes were changed less than 2 dB, and 30 dB sidelobes were changed 5 dB. An extensive stress analysis and thermal analysis were conducted and indicated a conservative mechanical design.

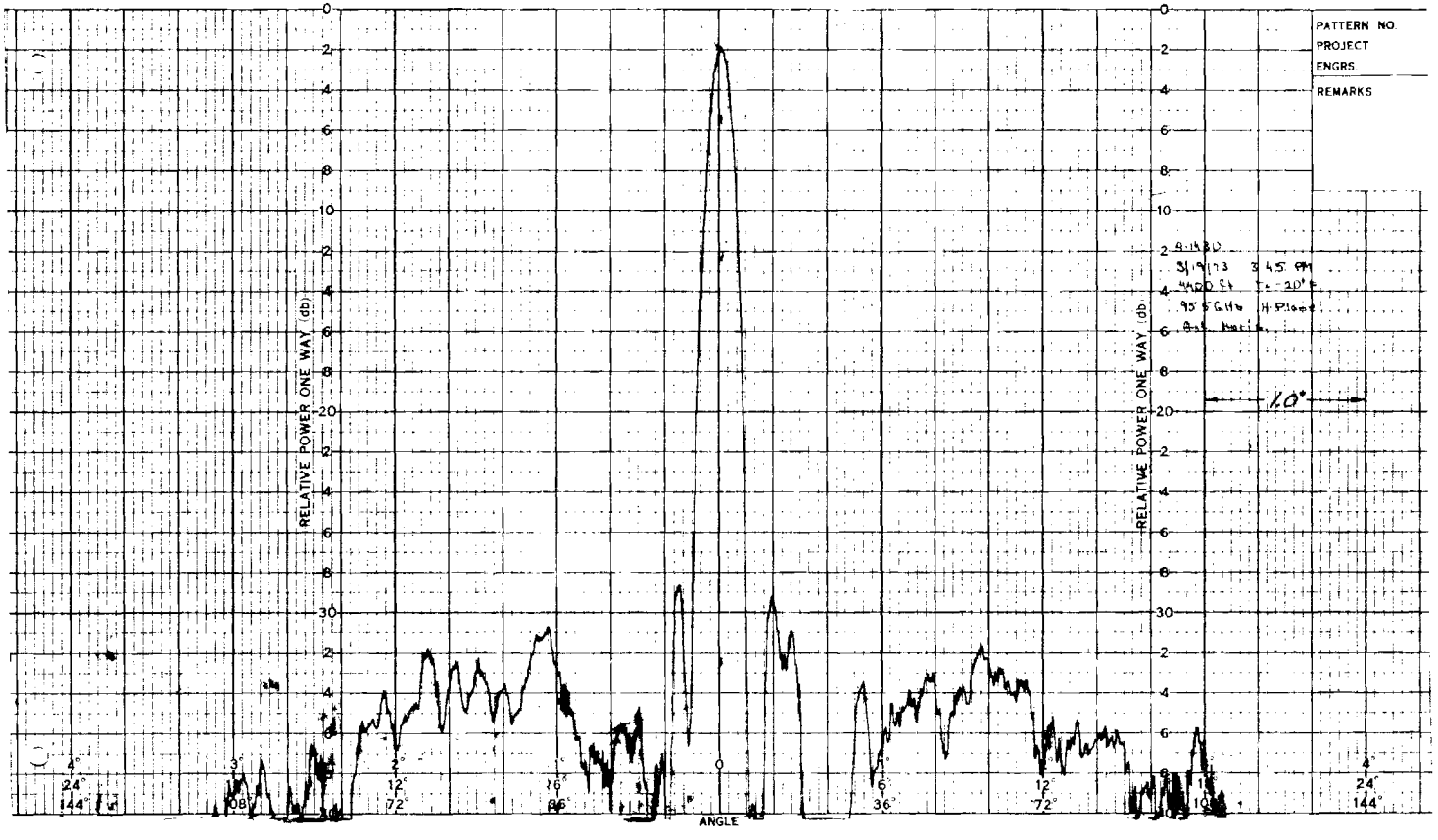

Figure 2. Expanded H-plane antenna pattern at 95.5 GHz on 4400 foot range with temperature at -20° F.

ANALYSIS OF AN ANISOTROPIC DIELECTRIC RADOME*

by

Donald G. Bodnar and Harold L. Bassett
Systems and Techniques Department
Engineering Experiment Station
Georgia Institute of Technology
Atlanta, Georgia 30332

ABSTRACT

A grooved-dielectric radome panel is analyzed in terms of an arbitrary direction of incidence on N planar slabs each of which is dielectrically anisotropic, homogeneous and lossless. Using this model for the grooved panel, transmission coefficients of 90 percent or greater over a 10:1 frequency band and over 0^{o} to 60^{o} incidence angle are predicted and demonstrated experimentally. Measurements are presented on two panels from 3 to 35 GHz.

I. INTRODUCTION

Reflections from radomes can be eliminated by smoothly changing the dielectric constant of the radome from a value of one at the inner and outer surfaces to an arbitrary value in the interior [1]. The possibility of physically realizing such radome performance is analyzed in this paper for a particular class of grooved dielectric panels shown in Figure 1. This panel is made by machining triangular grooves into both sides of a flat, solid piece of dielectric. It has been experimentally demonstrated [2] that the panel shown in Figure 1 can indeed have broadband performance. The purpose of this paper is to establish a theoretical basis for this performance, present some new experimental data, and to provide some new design data on this type of panel.

The radome technique described permits very broadband radomes to be realized that also operate over a wide range of incidence angles thus eliminating the need to "tune" for a particular frequency and/or incidence angle.

*This work was supported under Contract F33615-71-C-1694.

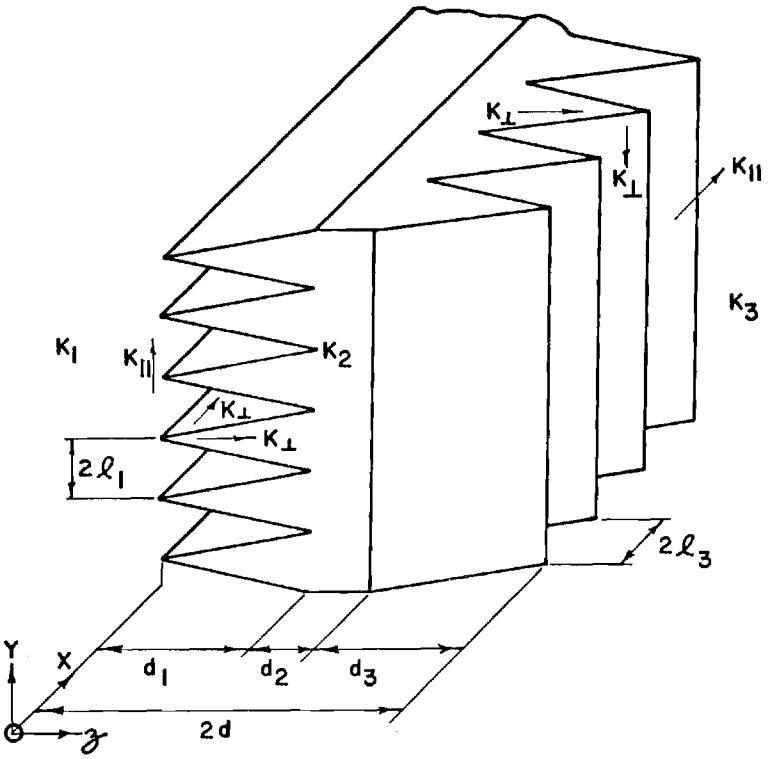

Figure 1. Grooved broadband panel design.

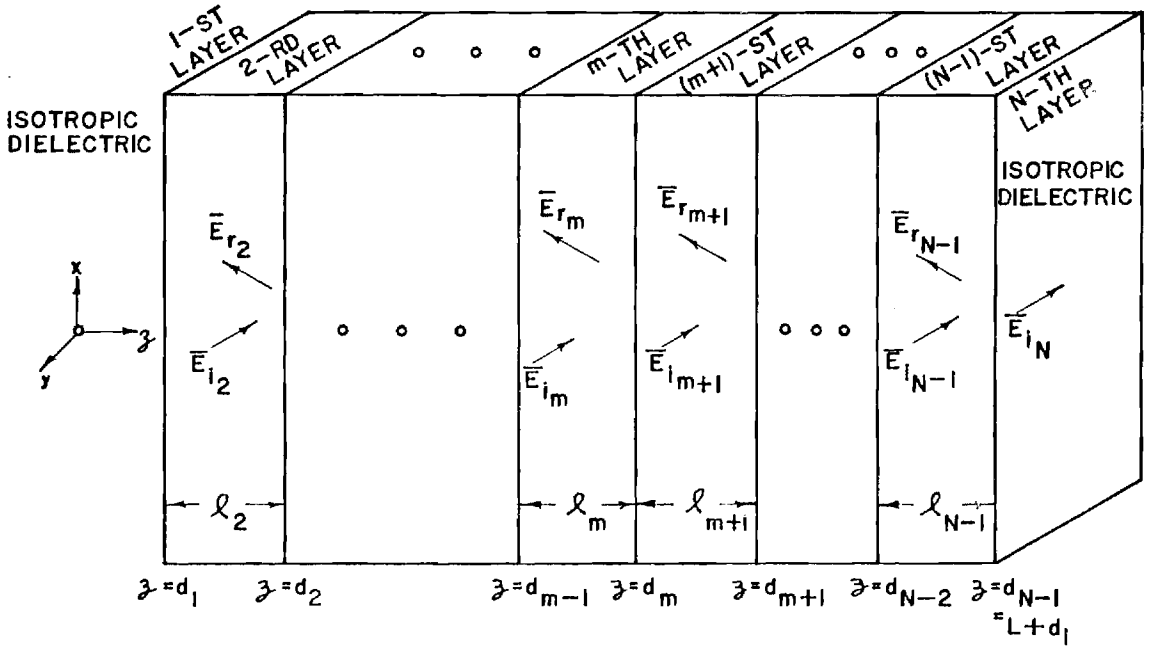

Figure 2, Geometry of homogeneous, anisotropic slabs.

II. MATHEMATICAL MODEL OF PANEL

The panel shown in Figure 1 is both dielectrically inhomogeneous and anisotropic since the dielectric properties vary both with position and with direction at a particular position. This panel was modeled as a series of slabs each perpendicular to the z axis as shown in Figure 2. Each slab is homogeneous but anisotropic in general, and each is intended to represent the medium parameters at the corresponding z location in Figure 1. Let there be a total of N slabs including the semi-infinite isotropic-dielectric regions on either side of the central slabs. The m-th slab starts at $z = d_{m-1}$ and ends at $z = d_m$. In the m-th slab the permeability is a scalar constant μ and the rectangular components of the permittivity tensor are given by

$$\bar{\bar{\varepsilon}}_m = \varepsilon_o \begin{bmatrix} \kappa_{x_m} & 0 & 0 \\ 0 & \kappa_{y_m} & 0 \\ 0 & 0 & \kappa_{z_m} \end{bmatrix} \tag{1}$$

where ε_o is the free space permittivity and κ_{x_m}, κ_{y_m} and κ_{z_m} are the dielectric constants in the various coordinate directions.

A series of ordinary and extraordinary waves [3, 4, 5] will typically be generated in each of the layers of the panel when a single plane wave is incident from the 1-st layer. A superscript o and e will be used to distinguish between ordinary and extraordinary components, respectively. As shown in Figure 2, the total electric field in the m-th layer will be composed of an incident field $\bar{E}_{i_m}$ traveling to the right and a reflected field $\bar{E}_{r_m}$ traveling to the left. Both of these electric fields will, in general, contain both ordinary and extraordinary components that travel in different directions with different velocities. Several ordinary and several extraordinary waves will be present in each $\bar{E}_{i_m}$ and each $\bar{E}_{r_m}$ if the optical axes

in each layer are arbitrarily oriented [5]. It can be shown that if (a) each slab is uniaxial (or isotropic), (b) the optical axis of each layer lies in the x-y plane, and (c) each optical axis is either parallel or perpendicular to all other optical axes then (1) only one ordinary and one extraordinary component exists for each $\bar{E}_{i_m}$ (similarly for $\bar{E}_{r_m}$) and (2) the incident and reflected waves in a medium have the same ordinary and extraordinary propagation constants, namely β_m^o and β_m^e, respectively. Assumptions (a), (b), and (c) are valid for the panel in Figure 1 and will be made in all that follows.

According to Born and Wolf [3] and to Jones [4], the electric flux density $\bar{D}$ of the ordinary wave in a uniaxial crystal (assumption (a) above) is perpendicular to the principal plane while $\bar{D}$ of the extraordinary wave lies in the principal plane. The principal plane is defined to be the plane containing the optic axis and the direction of propagation. Thus in each region there are four principal planes, one for the ordinary and the extraordinary components of both the incident and the reflected waves.

A rectangular coordinate system will now be established for each of these four components in terms of the principal planes. For brevity, let $\bar{n}_m$ represent any of the four directions of propagation vectors. Let $\bar{u}_{o_m}$ be a unit vector in the direction of the optical axis in the m-th region. Notice that $\bar{u}_{o_m}$ is independent of which of the four direction of propagation vectors is selected for $\bar{n}_m$. Let $\bar{u}_{\perp_m}$ be a unit vector perpendicular to both the optical axis and the direction of propagation $\bar{n}_m$ such that

$$\bar{u}_{\perp_m} = \frac{\bar{n}_m \times \bar{u}_{o_m}}{\left| \bar{n}_m \times \bar{u}_{o_m} \right|} \tag{2}$$

Notice that $\bar{u}_{\perp_m}$ depends on which direction of propagation is selected for $\bar{n}_m$. Finally, an orthogonal coordinate system will be completed by defining a unit vector $\bar{u}_{\parallel_m}$ in the principal plane such that

$$\bar{u}_{\parallel_m} = \frac{\bar{u}_{o_m} \times \bar{u}_{\perp_m}}{\left| \bar{u}_{o_m} \times \bar{u}_{\perp_m} \right|} \tag{3}$$

The unit vectors $\bar{u}_{o_m}$, $\bar{u}_{\perp_m}$, and $\bar{u}_{\parallel_m}$ form a right-handed rectangular coordinate system which is termed an optic axes coordinate system. The ordinary component of $\bar{D}$ is colinear with $\bar{u}_{\perp_m}$ and the extraordinary component of $\bar{D}$ lies in the principal plane. Since each layer is uniaxial, the dielectric constant is independent of direction in any plane transverse to the optic axis. Thus, by choosing $\bar{u}_{o_m}$, $\bar{u}_{\perp_m}$, and $\bar{u}_{\parallel_m}$ as the axes, the permittivity tensor can be reduced to diagonal form with the $\bar{u}_{\perp_m}$ and $\bar{u}_{\parallel_m}$ components of the tensor being identical. Thus, the components of $\bar{E}$ along the $\bar{u}_{o_m}$ and $\bar{u}_{\parallel_m}$ transfer into the extraordinary component of $\bar{D}$ and the component of $\bar{E}$ along $\bar{u}_{\perp_m}$ transfers into the ordinary component of $\bar{D}$.

The field components in each layer are represented in terms of the optic axes coordinate system. By matching the tangential electric and magnetic fields at each interface $z = z_m$ one obtains the following relationship between optical-axes coordinate-system components on each side of the interface

$$\bar{\bar{A}}_{m+1}(d_m) \cdot \bar{E}_{m+1} = \bar{\bar{A}}_m(d_m) \cdot \bar{E}_m \tag{4}$$

The $\bar{\bar{A}}$ tensor is a 4 x 4 tensor whose components are given in Appendix A while $\bar{E}_m$ and $\bar{E}_{m+1}$ are column vectors and

$$\bar{E}_m = \begin{bmatrix} E^i_{o_m} \\ E^i_{\perp_m} \\ E^r_{o_m} \\ E^r_{\perp_m} \end{bmatrix} \tag{5}$$

and $\bar{E}_{m+1}$ has the same form as $\bar{E}_m$ with m replaced by m+1. The subscripts o and $\perp$ represent components along $\bar{u}_{o_m}$ and $\bar{u}_{\perp_m}$, respectively, for the appropriate incident or reflected wave. By inverting (4) and by repeated multiplication, the electric fields inside the panel may be eliminated and one obtains

$$\bar{E}_N = \bar{\bar{C}} \cdot \bar{E}_1 \tag{6}$$

where

$$\bar{\bar{C}} = \bar{\bar{B}}_{N-1} \cdot \bar{\bar{B}}_{N-2} \cdot \bar{\bar{B}}_{N-3} \cdots \bar{\bar{B}}_2 \cdot \bar{\bar{B}}_1 \tag{7}$$

and

$$\bar{\bar{B}}_m = \bar{\bar{A}}_{m+1}^{-1}(d_m) \cdot \bar{\bar{A}}_m(d_m) \tag{8}$$

Usually the incident field is known and the transmitted and reflected fields must be found. This can be done by partitioning (6) and solving the resulting equations. One then obtains

$$\bar{E}_r = - \bar{\bar{F}}_4^{-1} \cdot \bar{\bar{F}}_3 \cdot \bar{E}_i \tag{9}$$

$$\bar{E}_t = (\bar{\bar{F}}_1 - \bar{\bar{F}}_2 \cdot \bar{\bar{F}}_4^{-1} \cdot \bar{\bar{F}}_3) \cdot \bar{E}_i \tag{10}$$

where

$$\bar{\bar{F}}_1 = \begin{bmatrix} C_{11} & C_{12} \\ C_{21} & C_{22} \end{bmatrix} \qquad \bar{\bar{F}}_2 = \begin{bmatrix} C_{13} & C_{14} \\ C_{23} & C_{24} \end{bmatrix}$$

$$\bar{\bar{F}}_3 = \begin{bmatrix} C_{31} & C_{32} \\ C_{41} & C_{42} \end{bmatrix} \qquad \bar{\bar{F}}_4 = \begin{bmatrix} C_{33} & C_{34} \\ C_{43} & C_{44} \end{bmatrix} \tag{11}$$

and the C's in (11) are the elements of $\overline{\overline{C}}$, and

$$\overline{E}_i = \begin{bmatrix} E^i_{o_1} \\ E^i_{\perp_1} \end{bmatrix} \qquad \overline{E}_t = \begin{bmatrix} E^i_{o_N} \\ E^i_{\perp_N} \end{bmatrix} \qquad \overline{E}_r = \begin{bmatrix} E^r_{o_1} \\ E^r_{\perp_1} \end{bmatrix} \tag{12}$$

The incident, $\overline{E}_i$ reflected $\overline{E}_r$ and transmitted $\overline{E}_t$ fields in (12) are specified in terms of optic axis coordinate systems. For more convenient usage they need to be expressed in terms of rectangular coordinate components. If the incident field in rectangular components in medium 1 is given by

$$\overline{E}_i = (E_x, E_y, E_z) \tag{13}$$

then

$$E^i_{o_1} = E_x \cos \theta_1 + E_y \sin \theta_1 \tag{14}$$

$$E^i_{\perp_1} = E_x u^i_{x\perp_1} + E_y u^i_{y\perp_1} + E_z u^i_{z\perp_1} \tag{15}$$

The angle θ_1 is the orientation of the optic axis in medium 1 with respect to the x axis. Since medium 1 is isotropic θ_1 may be arbitrarily set parallel or perpendicular to the other optic axes. A similiar conversion can be made to convert $\overline{E}_t$ and $\overline{E}_r$ to rectangular components.

The dielectric properties of the panel in Figure 1 were modeled by use of a semi-infinite strip-array analysis [2, 6]. The dielectric constant for perpendicular polarization (see Figure 1) which represents K_y and K_z for region d_1 of Figure 1 is given by the zero of the following function:

$$f_\perp(K_\perp) = -\frac{\pi}{2} + A\sqrt{K_2 - K_\perp} + \tan^{-1}\left[\sqrt{\frac{K_2 - K_\perp}{K_\perp - K_1}} \coth\left(B\sqrt{K_\perp - K_1}\right)\right] \tag{16}$$

where

$$A = 2\pi \frac{w}{\ell_1} \frac{\ell_1}{\lambda_o} \tag{17}$$

$$B = 2\pi \left(1 - \frac{w}{\ell_1}\right) \frac{\ell_1}{\lambda_o} \tag{18}$$

and w is the width of the strip at the z location of interest. The dielectric constant for parallel polarization which represents K_y for region d_1 of Figure 1 is given by the zero of the following function:

$$f_{\|}(K_{\|}) = A\sqrt{K_2 - K_{\|}} - \tan^{-1}\left[\frac{K_2\sqrt{K_{\|} - K_1}}{K_1\sqrt{K_2 - K_{\|}}} \tanh\left(B\sqrt{K_{\|} - K_1}\right)\right] \tag{19}$$

and A and B are defined as above. Equations 16 and 19 can be solved using Muller's method, Newton-Raphson or other techniques. By using an appropriate change in terms, (16) and (19) can be used to determine the K's of region d_3 of Figure 1.

The propagation constant of the ordinary wave in the m-th medium is given by

$$\beta_m^o = k_o\sqrt{K_{z_m}} \tag{20}$$

while that for the extraordinary wave is the solution of [7]

$$\begin{aligned}
&(\beta_{m+1}^2 - K_{y_{m+1}} k_o^2)(\beta_{m+1}^2 - K_{z_{m+1}} k_o^2) n_{x_m}^2 K_{x_{m+1}} \\
&+(\beta_{m+1}^2 - K_{z_{m+1}} k_o^2)(\beta_{m+1}^2 - K_{x_{m+1}} k_o^2) n_{y_m}^2 K_{y_{m+1}} \\
&+(\beta_{m+1}^2 - K_{x_{m+1}} k_o^2)(\beta_{m+1}^2 - K_{y_{m+1}} k_o^2) \\
&\cdot\left(\frac{\beta_{m+1}^2}{\beta_m^2} - n_{x_m}^2 - n_{y_m}^2\right) K_{z_{m+1}} = 0
\end{aligned} \tag{21}$$

Since all quantities of interest in (21) are known in the first region they may be determined for all media to the right of it. The direction of propagation in each region can be determined from that in the first region by

$$n_{x_{m+1}} = \frac{\beta_m}{\beta_{m+1}} n_{x_m}$$

$$n_{y_{m+1}} = \frac{\beta_m}{\beta_{m+1}} n_{y_m}$$

$$n_{z_{m+1}} = + \sqrt{1 - n^2_{x_{m+1}} - n^2_{y_{m+1}}} \qquad (22)$$

III. COMPARISON OF MEASURED AND PREDICTED PERFORMANCE

The initial performance predictions were based on the conditions for which the Richmond WKB solution is valid [1] for plane wave transmission through inhomogeneous layers. For a lossless panel, for any angle of incidence, total transmission of power is obtained; the insertion phase delays of the parallel and perpendicular components are equal, and the phase of the transmitted wave depends only on the average value of $\sqrt{K(z) - \sin^2\theta}$ in the panel of thickness d.

The main problem with applying these results was that of realizing a practical structure that has the required variation, $K(z)$, of dielectric constant. That is

(1) $K(0) = 1.0$ (incident point),

(2) $K(d) = 1.0$ (exit point), and

(3) $\left| \frac{dK(z)}{dz} \right| \ll 2k[K(z) - \sin^2\theta]^{3/2}$

as required by Richmond's WKB solution.

In utilizing these results for the panel in Figure 1, additional design

data were required. As previously reported [2], the spacing restriction is:

$$2\ell/\lambda_o = \frac{1}{\sqrt{\kappa_2} + \sqrt{\kappa_1}\ |\sin\theta|}\ , \tag{23}$$

where

θ_1 = angle of incidence,
κ_1 = 1 (dielectric constant of free space)
κ_2 = dielectric constant of panel material, and
2ℓ = center-to-center spacing of the strips.

There was also a restriction on the rate of change of the dielectric constant with distance. The restriction for which the WKB solution is valid is given by

$$\left|\frac{d\kappa}{dz}\right| << \frac{4\pi}{\lambda_o}\left[\kappa(z) - \sin^2\theta\right]^{3/2}, \tag{24}$$

where

$\kappa(z)$ = real part of complex permittivity function, and
λ_o = operating free-space wavelength.

By utilizing Equations 23 and 24, design parameters were calculated for a broadband panel and these data are tabulated in Table I. For a center-to-center spacing of the grooves of 0.26-inch the upper frequency limit would be 18 GHz (essentially the upper frequency limit is controlled by the groove spacing.) The lower frequency limit is controlled by the depth of the grooves, d_1, and for 2 GHz to 18 GHz operation, this value would be 5.8 inches. This thickness was impractical and it was decided to use a panel thickness of 1.5 inches with 0.625-inch groove depths on each side of the panel. The panel did have an upper frequency cut-off near 18.0 GHz while the lower frequency cut-off was near 4.0 GHz. This panel is referred to as Panel No. 1 in the section on measured results. Another Panel, No. 2, was fabricated with a groove spacing of 0.125-inch and data are also presented on this panel. Both panels were made of Rexolite.

TABLE I

Calculated Parameters for Broadband Panel

f_{max}, f_{min} (GHz)	ℓ (Inches)*	$d_1 min$ (Inches)
2	1.20042	5.78973
4	.60021	2.89487
6	.40014	1.92991
8	.30011	1.44743
10	.24008	1.15795
12	.20007	.96496
14	.17149	.82710
16	—	—
18	.13338	.64330
20	—	—
22	—	—
24	.10004	.48248
26	—	—
28	—	—
30	.08003	.38598
32	—	—
34	—	—
36	.06669	.32165

*Note that ℓ is the half-spacing of the strips; the center-to-center spacing is 2ℓ.

A. Measurement Technique

A microwave phase shift bridge free-space technique was employed to determine the broadband panel insertion phase shift and insertion loss as functions of frequency, incidence angle and polarization. A Scientific-Atlanta phase/amplitude receiver was used in the measurements to obtain the panel transmission data.

A reference flat panel was inserted between the two horns in the sample arm of the phase shift bridge and the system was adjusted and calibrated so that the reference test panel transmission properties approached those of calculated data for a theoretical flat panel. Once the reference flat panel measurements were completed, the broadband panel was inserted into the test fixture and the transmission properties were recorded. These data were taken at 1.0 GHz intervals from 2.0 GHz to 24 GHz on Panel No. 1 and from 2.0 GHz to 40 GHz on Panel No. 2.

B. Measured Results

The panel transmission data are presented for the 0^{o} and 60^{o} incidence angle cases only. The data for the angles between 0^{o} and 60^{o} were measured, and since these data fall within the cases plotted, it was felt unnecessary to present each data point. Thus, only the extreme cases are presented here. It also reduces considerably the number of plots required to define each panel.

The transmission data for Panel No. 1 are presented in Table II. Both the measured and predicted values are shown. Note that the transmission properties of Panel No. 1 are excellent to about 20 GHz. For vertical polarization (the perpendicular polarization case), the insertion loss changes drastically near 20 GHz. On the low end of the frequencies tested, the panel did not transmit satisfactorily below 4.0 GHz. Panel No. 1 operated satisfactorily from 4 GHz to 18 GHz.

The transmission data for Panel No. 2 are presented in Table III. Again, only the 0^{o} and 60^{o} incidence angle cases are shown. The panel had good transmission properties from 4 GHz to 36 GHz. Transmission properties of the vertical polarization case, which is the worst case, are tabulated from 3 GHz to 35 GHz. Spot checks of horizontal polarization were made which indicated that the panel transmission properties are better for

TABLE II

COMPARISON OF MEASURED AND PREDICTED TRANSMISSION LOSS AND INSERTION PHASE DELAY FOR PANEL NUMBER 1

Freq. (GHz)	0° Incidence				60° Incidence			
	$\lvert T_{\parallel} \rvert$ (dB)	$\angle T_{\parallel}$ (degrees)	$\lvert T_{\perp} \rvert$ (dB)	$\angle T_{\perp}$ (degrees)	$\lvert T_{\parallel} \rvert$ (dB)	$\angle T_{\parallel}$ (degrees)	$\lvert T_{\perp} \rvert$ (dB)	$\angle T_{\perp}$ (degrees)
3	0.50*	41	0.40	44	0.20	70	3.10	62
	0.44	42	0.44	42	0.02	71	2.89	59
4	-0.15	55	0.10	55	-0.40	94	1.60	75
	0.06	57	0.06	57	0.07	95	1.54	75
9	-0.22	135	-0.22	142	-0.25	-145	-0.14	-157
	0.02	135	0.02	135	0.10	-147	0.10	-163
15	-0.15	-128	0.00	-134	-0.03	-7	0.30	-18
	0.00	-130	0.00	-130	0.06	0	0.46	-19
20	-0.10	-45	-0.15	-45	-0.30	125	-0.05	120
	0.00	-46	0.00	-46	0.00	128	0.14	104
25	0.00	46	-0.05	41	0.40	-110	-12.9	-50
	0.00	42	0.00	42	0.09	-97	0.03	-125
30	-	-	-	-	-	-	-	-
	0.00	137	0.00	137	0.04	45	0.14	14
35	-	-	-	-	-	-	-	-
	0.00	-122	0.00	-122	0.04	-164	0.03	161

*Upper figures are measured values, lower figures are predicted values.

TABLE III

COMPARISON OF MEASURED AND PREDICTED TRANSMISSION LOSS AND INSERTION PHASE DELAY FOR PANEL NUMBER 2

Freq. (GHz)	0° Incidence				60° Incidence			
	$\lvert T_{\parallel} \rvert$ (dB)	$\angle T_{\parallel}$ (degrees)	$\lvert T_{\perp} \rvert$ (dB)	$\angle T_{\perp}$ (degrees)	$\lvert T_{\parallel} \rvert$ (dB)	$\angle T_{\parallel}$ (degrees)	$\lvert T_{\perp} \rvert$ (dB)	$\angle T_{\perp}$ (degrees)
3	0.50*	45	0.35	43	0.00	74	2.85	63
	0.44	42	0.44	42	0.02	71	2.89	59
4	-0.20	58	0.08	59	-0.25	102	1.30	79
	0.06	57	0.06	57	0.07	95	1.55	74
9	-0.10	137	-0.20	137	0.10	-136	0.00	-152
	0.01	134	0.01	134	0.09	-148	0.11	-165
15	0.05	-128	0.05	-125	0.05	-11	0.25	-13
	0.00	-134	0.00	-134	0.06	-6	0.43	-25
20	0.05	-48	-0.10	-49	0.20	130	0.00	110
	0.00	-57	0.00	-57	0.01	114	0.16	89
25	0.10	32	0.10	31	0.60	-93	0.60	-125
	0.00	21	0.00	21	0.04	-124	0.01	-153
30	-	-	0.10	116	-	-	0.35	-7
	0.00	101	0.00	101	0.07	0	0.05	-34
35	-	-	0.10	-140	-	-	0.10	171
	0.00	-177	0.00	-177	0.00	127	0.10	88

*Upper figures are measured values, lower figures are predicted values.

horizontal polarization than for vertical polarization. The agreement of phase angles was worse for Panel No. 2 than for Panel No. 1 since the tops of the wedges of Panel No. 2 were blunted instead of sharp as in the mathematical model.

The computer analysis program, which is being presented in this paper, was formulated during the panel measurement program. The analysis verifies the measured data as indicated in Table II and III. By having this program, one can analyze the transmission properties of any anisotropic dielectric panel.

Appendix A

AMPLITUDE COEFFICIENT TENSOR

The tensors $\overline{\overline{A}}_m$ and $\overline{\overline{A}}_{m+1}$ have the same form only the subscript are different. The argument d_m of these tensor functions, however, is the same for both. For an argument d, the form of these tensors is as follows:

$$\overline{\overline{A}}_m(d) = \begin{bmatrix} A_{11} & A_{12} & A_{13} & A_{14} \\ A_{21} & A_{22} & A_{23} & A_{24} \\ A_{31} & A_{32} & A_{33} & A_{34} \\ A_{41} & A_{42} & A_{43} & A_{44} \end{bmatrix}$$

where

$$A_{11} = \left(\cos\ \theta_m + C_{\|i_m}\ u^i_{x\|_m}\right) e^e_m(d)$$

$$A_{12} = u^i_{x\perp_m}\ e^o_m(d)$$

$$A_{13} = \left(\cos\ \theta_m + C_{\|r_m}\ u^r_{x\|_m}\right) e^{e^*}_m(d)$$

$$A_{14} = u^{r}_{x_{\perp_m}} \; e^{o^*}_{m}(d)$$

$$A_{21} = \left(\sin \theta_m + C_{\|i_m} \; u^{i}_{y\|_m}\right) e^{e}_{m}(d)$$

$$A_{22} = u^{i}_{y_{\perp_m}} \; e^{o}_{m}(d)$$

$$A_{23} = \left(\sin \theta_m + C_{\|r_m} \; u^{r}_{y\|_m}\right) e^{e^*}_{m}(d)$$

$$A_{24} = u^{r}_{y_{\perp_m}} \; e^{o^*}_{m}(d)$$

$$A_{31} = \beta^{e}_{m} \left[-n^{e}_{zi_m} \sin \theta_m + C_{\|i_m} \left(n^{e}_{yi_m} \; u^{i}_{z\|_m} - n^{e}_{zi_m} \; u^{i}_{y\|_m}\right)\right] e^{e}_{m}(d)$$

$$A_{32} = \beta^{o}_{m} \left(n^{o}_{yi_m} \; u^{i}_{z_{\perp_m}} - n^{o}_{zi_m} \; u^{i}_{y_{\perp_m}}\right) e^{o}_{m}(d)$$

$$A_{33} = \beta^{e}_{m} \left[-n^{e}_{zr_m} \sin \theta_m + C_{\|r_m} \left(n^{e}_{yr_m} \; u^{r}_{z\|_m} - n^{e}_{zr_m} \; u^{r}_{y\|_m}\right)\right] e^{e^*}_{m}(d)$$

$$A_{34} = \beta^{o}_{m} \left(n^{o}_{yr_m} \; u^{r}_{z_{\perp_m}} - n^{o}_{zr_m} \; u^{r}_{y_{\perp_m}}\right) e^{o^*}_{m}(d)$$

$$A_{41} = \beta^{e}_{m} \left[n^{e}_{zi_m} \cos \theta_m + C_{\|i_m} \left(n^{e}_{zi_m} \; u^{i}_{x\|_m} - n^{e}_{xi_m} \; u^{i}_{z\|_m}\right)\right] e^{e}_{m}(d)$$

$$A_{42} = \beta^{o}_{m} \left(n^{o}_{zi_m} \; u^{i}_{x_{\perp_m}} - n^{o}_{xi_m} \; u^{i}_{z_{\perp_m}}\right) e^{o}_{m}(d)$$

$$A_{43} = \beta_m^e \left[n_{zr_m}^e \cos \theta_m + C_{\parallel r_m} \left(n_{zr_m}^e \, u_{x\parallel_m}^r - n_{xr_m}^e \, u_{z\parallel_m}^r \right) \right] e_m^{e^*}(d)$$

$$A_{44} = \beta_m^o \left(n_{zr_m}^o \, u_{x\perp_m}^r - n_{xr_m}^o \, u_{z\perp_m}^r \right) e_m^{o^*}(d)$$

To simplify manipulations, the following terms were defined. Let

$$e_m^o(d) = e^{-j\beta_m^o \, n_{zi_m}^o \, d}$$

$$e_m^e(d) = e^{-j\beta_m^e \, n_{zi_m}^e \, d}$$

Then

$$e_{m+1}^o(d_m) = e^{-j\beta_{m+1}^o \, n_{zi_{m+1}}^o \, d_m}$$

$$e_{m+1}^e(d_m) = e^{-j\beta_{m+1}^e \, n_{zi_{m+1}}^e \, d_m}$$

and

$$e_m^o(d_m) = e^{-j\beta_m^o \, n_{zi_m}^o \, d_m}$$

$$e_m^e(d_m) = e^{-j\beta_m^e \, n_{zi_m}^e \, d_m}$$

The parallel components of the field were eliminated by using $\bar{n} \cdot \bar{D} = 0$ thus obtaining

$$E^{i}_{\parallel_m} = C_{\parallel i_m} E^{i}_{o_m}$$

where

$$C_{\parallel i_m} = - \frac{n^{e}_{xi_m} K_{x_m} \cos \theta_m + n^{e}_{yi_m} K_{y_m} \sin \theta_m}{n^{e}_{xi_m} K_{x_m} u^{i}_{x\parallel_m} + n^{e}_{yi_m} K_{y_m} u^{i}_{y\parallel_m} + n^{e}_{zi_m} K_{z_m} u^{i}_{z\parallel_m}}$$

and

$$E^{r}_{\parallel_m} = C_{\parallel r_m} E^{r}_{o_m}$$

where

$$C_{\parallel r_m} = - \frac{n^{e}_{xr_m} K_{x_m} \cos \theta_m + n^{e}_{yr_m} K_{y_m} \sin \theta_m}{n^{e}_{xr_m} K_{x_m} u^{r}_{x\parallel_m} + n^{e}_{yr_m} K_{y_m} u^{r}_{y\parallel_m} + n^{e}_{zr_m} K_{z_m} u^{r}_{z\parallel_m}}$$

The angle θ_m is used to specify the orientation of the optic axis with respect to the x axis in the m-th layer as

$$\bar{u}_{o_m} = \cos \theta_m \bar{a}_x + \sin \theta_m \bar{a}_y + 0 \bar{a}_z$$

REFERENCES

1. J. H. Richmond, "The WKB Solution for Transmission Through Inhomogeneous Plane Layers," IRE Trans. on Antennas and Propagation, Vol. AP-10, pp. 472-473, July 1962.

2. H. L. Bassett and G. K. Huddleston, "Broadband Radome Techniques," Interim Report Number 1, Georgia Tech Project A-1333, Atlanta, Georgia, February 1973.

3. M. Born and E. Wolf, Principles of Optics, New York: Pergamon Press, 1964, pp. 665-681.

4. D. S. Jones, The Theory of Electromagnetism, New York: Pergamon Press, 1964, pp. 329-332.

5. J. Strong, Concepts of Classical Optics, San Francisco: W. H. Freeman, 1958, pp. 128-133.

6. T. Morita and S. B. Cohn, "Microwave Lens Matching by Simulated Quarter-Wave Transformers," IRE Trans. on Antennas and Propagation, Vol. AP-4, pp. 33-39, January 1956.

7. R. E. Collin, Field Theory of Guided Waves, New York: McGraw Hill, 1960, pp. 97-102.

A-1551

FINAL TECHNICAL REPORT

95 GHz COBRA LEADING EDGE ANTENNA SYSTEM

EES/GIT PROJECT A-1551

Prepared for

UNITED STATES ARMY

FRANKFORD ARSENAL

PHILADELPHIA, PA. 19137

UNDER

CONTRACT DAAA25-73-C-0648

by

D. G. Bodnar and R. M. Goodman, Jr.

15 April 1974

Engineering Experiment Station

GEORGIA INSTITUTE OF TECHNOLOGY

Atlanta, Georgia

GEORGIA INSTITUTE OF TECHNOLOGY
Engineering Experiment Station
Atlanta, Georgia

Final Technical Report
EES/GIT Project A-1551

95 GHz COBRA LEADING EDGE ANTENNA SYSTEM

by

D. G. Bodnar and R. M. Goodman, Jr.

Contract Number DAAA25-73-C-0648

15 April 1974

Prepared for

United States Army
Frankford Arsenal
Philadelphia, Pennsylvania 19137

ABSTRACT

An antenna concept has been developed and a conceptual design performed for a 95 GHz antenna system to be located in a modified stub-wing of an AH-1G Cobra helicopter. The antenna system consists of three antennas: two 18-inch diameter geodesic lenses and one 9-inch diameter Cassegrain reflector. One lens is placed in each stub-wing and each lens scans a 0.5^{o} beam (2^{o} beam in the non-scan plane) over a 60^{o} sector from dead ahead. These lenses provide search coverage over a 120^{o} sector. Target tracking and identification is achieved by a conically scanned Cassegrain antenna located in one of the wings. Using off-the-shelf receiver and transmitter components, the proposed system should provide detection and tracking out to 12 to 18 km. The existing stub-wing must be approximately doubled in size in order to accommodate the antennas. This wing modification will not significantly alter the aircraft performance since the stub-wing is not an aerodynamic lifting surface.

ACKNOWLEDGEMENTS

The authors acknowledge with gratitude the contributions of Drs. E. K. Reedy and R. D. Hayes of Georgia Tech in establishing the radar requirements for the proposed 95 GHz radar. These requirements are essential input for specifying the performance required from the leading edge antenna.

TABLE OF CONTENTS

LIST OF FIGURES

LIST OF TABLES

I. INTRODUCTION

A. Purpose of Study

The objective of the study performed under this contract was to develop an antenna concept and to perform a conceptual design for a 95 GHz antenna system which could be located in a modified stub-wing of an AH-1G Cobra helicopter. This antenna system, when combined with an appropriate radar, should provide target detection, acquisition, tracking and identification out to 12 to 18 km. Targets of interest include tanks, tracked vehicles, trucks, jeeps, and personnel. The antenna location was selected by Frankford Arsenal after considering a number of alternative locations. The nose of the helicopter is, of course, a desirable location for the antenna. However, future plans call for using the nose for weapons and other sensors, thus, this location will not be available for the radar antenna. Other antenna locations considered by Frankford Arsenal included mounting arrays conformal to the nose of the helicopter, mounting the antenna in the shroud around the engine drive shaft above the pilot, mounting in a pod which would be located either under one of the wings or between the skids, and mounting in the stub-wing. An initial look at mounting the antenna conformal with the nose or locating a phased array in the leading edge indicated that the cost and development risks would be high for a millimeter antenna. Mounting in the shroud area did not afford sufficient room for packaging a practical scanning antenna. Mounting the antenna in a canister and placing the canister on one of the stub-wings would reduce the fire power of the aircraft, and so, was deemed unsatisfactory. Mounting under the belly of the helicopter between the skids presents a serious clearance problem when the aircraft makes a hard landing. In addition, the landing struts block the antenna's view. Hence, this location was ruled out. The stub-wing location was selected as the best location for the following reasons. (1) Sufficient room is available, with some wing modification, for mounting an antenna in the wing. (2) This location will not reduce the fire power of the aircraft. (3) Changing this wing will not drastically alter the aerodynamic performance of the vehicle.

A geodesic lens was selected as the candidate antenna for study because of its excellent wide-angle scan capabilities and because it was felt that such an antenna could be developed at millimeter frequencies without great risk. Initially three frequencies were selected for examination, namely 35 GHz, 70 GHz, and 95 GHz. These frequencies were selected because atmospheric windows exist at these frequencies, and because of the availability of components at the frequencies. The majority of the emphasis in the program was placed at 95 GHz by Frankford Arsenal because of the improved resolution for a fixed antenna size that can be obtained at 95 GHz over the other frequencies, and because backscatter measurements indicated improved performance at 95 GHz over 70 GHz.

B. Background

Operation of small aircraft in the battlefield environment of a mid-intensity conflict places a set of requirements on the electromagnetic sensors which generally cannot be satisfied by equipment in the Army's inventory at this time. The aircraft will most likely fly in a nap-of-the-earth mode to reduce the possibility of detection by enemy tanks and track mounted weapons. Weather conditions encountered in the mid-intensity type conflict vary widely. Daily conditions vary from clear skies to heavy overcast of nimbo-stratus clouds and from fog to heavy rains of 25 mm/hr. In addition, the need exists to operate at night with no light as well as in daylight periods of full sun intensity. It currently appears that increased capability is needed by the aircraft in order that it can survive as well as conquer the opposition by improved fire power.

The study reported in the following sections has been directed toward the determination of antenna apertures which can be used to direct electromagnetic energy at the battlefield and have the best potential for assisting in locating and identifying targets. In addition, a location on the aircraft must be selected which does not interfere with other sensors and is of a configuration which does not reveal the presence of another sensor.

A number of operational parameters must be chosen in order to establish a set of base-line requirements for the total sensor requirements which in turn influence the antenna aperture of the sensor. In this sense, not all parameters

of the system have been considered or studied, but only those which have influence on the aperture. A system study for a scout type of helicopter was performed by the Sensor Systems Division of Georgia Tech using internal funds. This study was undertaken in order to establish the technical requirements of a 95 GHz radar system needed to perform the scout mission. The study resulted from a request for a 95 GHz radar concept for a scout helicopter from Col. Wayne B. Davis of the Office of Chief of Research and Development, Department of the Army. The results of this radar system study were presented to Col. Davis in an informal report entitled "A Millimeter Radar Concept for Helicopter Application" by Bodnar, Reedy, Dyer, and Goodman dated January 1974. A good deal of this study also applies to the Cobra helicopter, and hence, helps establish the feasibility of a 95 GHz radar for the Cobra.

In view of the requirements for adverse weather and night operation, it appears that IR and optical wavelengths are less desirable than millimeter or centimeter wavelength radiation. Since a small, lightweight system is preferred, millimeter wavelengths appear a better choice than centimeter wavelengths. The availability of hardware and developed components and an examination of atmospheric transmission properties leads one to consider only 35, 70, or 95 GHz as potential operating frequencies. Systems operating at 70 GHz are less desirable since it has been shown [1,2] that there is an adverse effect caused by rain attenuation and backscattering at 70 GHz as compared to either 35 or 95 GHz.

In application to the fire-control weapon use, it will be desirable that the antenna perform a true area search over an azimuth sector of $\pm$ 60 degrees from dead-ahead and over a range sector from 1500 meters to 18,000 meters. In addition, when a particular target has been identified, it will be required to track this target in a range sector from 6,000 meters to 1,000 meters for the purpose of munition delivery. It is desired to have a small enough azimuth beamwidth that targets separated under standard deployment procedures can be resolved by the radar. For example, a beam one degree wide will illuminate a section 17.4 meters wide at 1000 meters range and 314 meters wide at 18,000 meters range. This is about the maximum beamwidth that could be used in the anticipated mid-intensity conflict.

The range resolution of a radar is controlled by the pulse length of the transmitted energy. For example, during a nap-of-the-earth flight, a 100 ns

pulse will illuminate a 15 meter strip on the ground. The radar prf will establish the number of pulses that hit an illuminated area per second if the antenna is stationary. The number of pulses required to illuminate a target to insure a sufficiently low false alarm rate must be combined with how often this information must be up-dated in order to determine the prf. Thus the scan rate of the radiated beam must be determined from aircraft speed, false alarm rate, azimuth beamwidth, pulse length, and prf.

During the short range weapon delivery operation, tracking of the target is required for accurate delivery of the munition. One of the major assets of small aircraft and helicopters is the extreme maneuverability of the ship. However, the wide range of aircraft attitudes places an extreme burden on the stabilization and pointing of the radar antenna. For example, the nose down attitude of the Cobra changes as a function of speed. Climb angles of 27°, descent angles of 40°, and turn angles of 30° are encountered in extreme maneuvers. In addition, an azimuth yaw of 5° at a cyclic rate of 1/6 Hz and a pitch variation of 5° at 1/6 Hz are observed in the Cobra helicopter.

The following sections present the results of a conceptual design study of a millimeter antenna system of an AH-1G Cobra Helicopter that is capable, when integrated with an appropriate radar, of achieving target location, identification, and tracking for munition delivery in a mid-intensity battlefield environment.

II. CANDIDATE ANTENNA CONCEPTS

The antenna work performed during this study was oriented toward the use of millimeter geodesic lens antennas in or on the stub wings of the AH-1G Cobra helicopter. A preliminary study was made of other types of antennas such as waveguide, stripline arrays, and phased arrays. The cost and/or development risk associated with these alternate antennas was deemed unreasonably high. Hence, an antenna type which had the potential of providing the desired performance at millimeter frequencies with low risk was selected by Frankford Arsenal for this study.

The basic type of antenna considered is a geodesic Luneberg lens. The geodesic Luneberg lens is a waveguide analog of a planar slice through a three-dimensional Luneberg lens [3]. The geodesic Luneberg lens has the property that a point-source feed on its periphery is transformed into a line source diametrically opposite the feed point. Thus the geodesic lens provides collimation of energy in one plane. Collimation of energy in the other plane can be obtained, for example, through the use of a parabolic cylinder fed by the line source output of the geodesic lens. Geodesic lenses are excellent scanning antennas even at millimeter wavelengths. Geodesic lenses have been built at Georgia Tech for X-band to V-band (70 GHz) [4,5,6]. They are very broadband devices that typically operate over an entire waveguide band. Thus they are compatible with Doppler signal processing and frequency agile transmitters.

A line drawing of the AH-1G Cobra helicopter is shown in Figure 1. The stub-wings are located on both sides of the helicopter behind the pilot's seat. The dimensions of a stub-wing are given in Figure 2. The wing is composed of three I beams that are perpendicular to the fuselage center line and which are covered by an airfoil. Each wing may be detached as a unit from the aircraft fuselage. The stub-wing is used as an attachment point for weapons and is not an aerodynamic lifting surface.

The decision to try to utilize the leading-edge location for the antennas was reached by Frankford Arsenal after considering a number of alternate

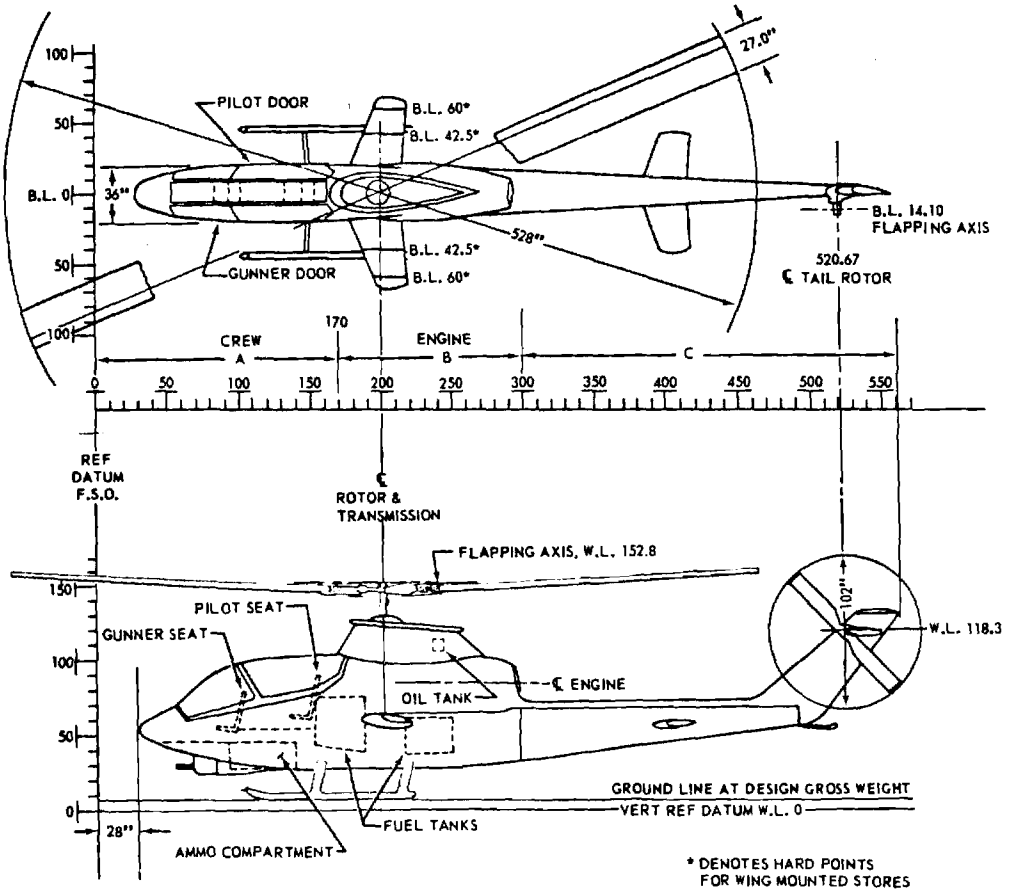

Figure 1. The AH-1G Cobra helicopter.*

*Figure taken from Department of the Army Technical Manual TM 55-1520-221-10, 19 June 1971, p. 12-3.

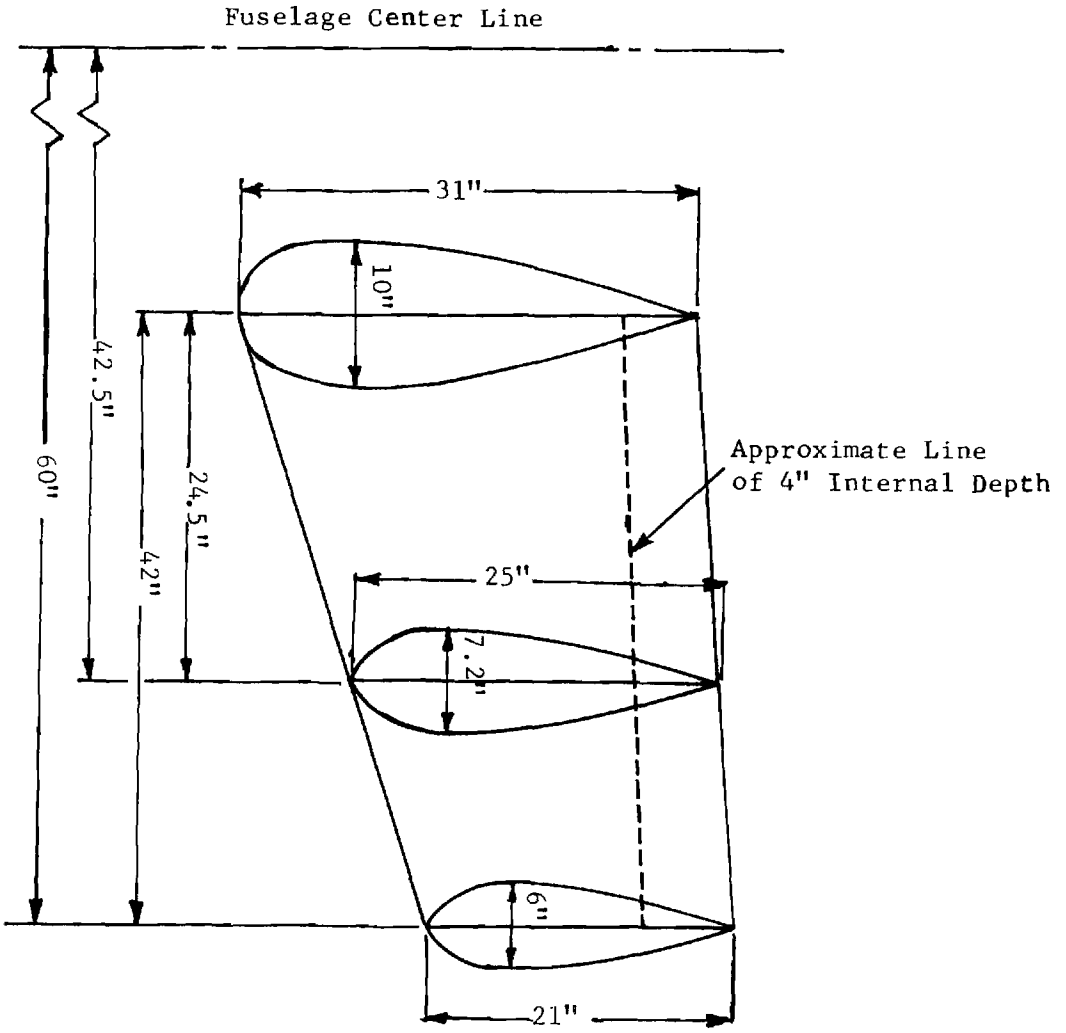

Figure 2. Approximate dimensions of AH-1G stub-wing.

locations. Some of the advantages of the leading edge location are (1) space is available in the wings for the antennas, (2) fire power is not compromised, and (3) only a small drag increase is expected by the resulting wing modification. The stub-wings on the attack helicopter are actually beams on which weapon stores are hung. An airfoil is placed around the beams to streamline their shape. They are not aerodynamic lifting surfaces, however, and so modifying their shape will not drastically affect aircraft performance.

Two antennas, one in each wing, will be required for the target detection mode using the leading-edge location due to the optical blockage produced by the fuselage. Each geodesic lens will scan a 60^{o} sector on its side of the vehicle from dead ahead. It would of course be desirable for these antennas to provide both the sector search as well as the tracking function. A track-while-scan mode was considered for the antennas but was eliminated since an insufficient number of pulses is returned from the target to permit Doppler processing. It is believed that the Doppler signature will be very important in identifying targets and should be retained via an alternate approach.

Another approach for dual mode operation is to stop the scanner and look at the desired target for a short period of time and then resume scanning. The time required to stop (or start) an electromechanical scanner is on the order of 1/2 second. Thus the sector search will be off for an appreciable portion of time using this approach. Hence, this approach for dual mode operation is not recommended.

The approach finally selected involves the use of three antennas. The two geodesic lenses previously discussed are used for target detection only. A third antenna provides the tracking function. Some of the candidate antenna concepts that were considered in the process of arriving at the above recommended geometry are discussed in the next sections. Some of the characteristics desired by Frankford Arsenal for this antenna are listed in Table I.

A beamwidth of 1^{o} or less is desirable in azimuth for adequate target resolution and a 2^{o} beamwidth in elevation (possible with some shaping) should provide adequate ground coverage in the search mode. Range performance calculations, assuming off-the-shelf components, indicates that a 0.5^{o} azimuth beamwidth is required to achieve detection ranges in the order 12 to 18 km as

Table I

Antenna Performance Characteristics Desired
for the AH-1G Leading Edge Antenna System

Parameter	Nominal Value
Az BW	1^{o} maximum
Az Coverage (Scan sector)	120^{o} total
El Coverage	$15\text{-}20^{o}$ total
El BW	2^{o} plus shaping
Power	20 kw
Bandwidth	1 to 2 GHz
Frequency	35, 70, or 95 GHz
Scan rate	6-10 per sec
Pulse Length	50 n sec
prf	4 kHz
Dual Polarization	Desirable
Az and El tracking	Dead ahead only
Tracking Accuracy	1.2 mrad
Track While Scan	Desirable

desired. Thus the antenna must produce a 0.5^{o} by 2^{o} beam in the search mode. A $\csc^{2}\theta$ pattern should be used beyond 2^{o} to achieve proper ground coverage.

A. Large Aperture Approach

The aperture size in both the E- and H-planes is determined both by the available size for packaging the antenna and by the resolution requirements. The maximum size of the Cobra wing is roughly 10 inches high and 31 inches deep (front-to-back) as seen from Figure 2. However, the major portion of the wing is much smaller than this. The largest folded geodesic lens, non-gimbaled, which could be fitted into this envelope is about 15 to 25 inches in diameter.

The relationship between beamwidth, aperture size, and frequency was examined and is presented in Figure 3. A cosine shaped aperture distribution raised to the first power produces -23 dB sidelobes [7] while the cosine squared distribution produces -32 dB sidelobes. This range of sidelobe levels brackets those expected from the final antenna.

From Figure 3 it can be seen that the desired 0.5^{o} search beamwidth in azimuth requires an aperture of 50 inches at 35 GHz, 26 inches at 70 GHz and 18 inches at 95 GHz. The aperture required to produce a 2^{o} beam is one fourth the corresponding values for the 0.5^{o} beam. Operation at 95 GHz permits a smaller antenna for a fixed resolution than does operation at lower frequencies. However, the antenna is still large physically due to the narrowness of the beam that must be produced.

If the aperture is sufficiently large, the desired tracking resolution can be obtained from the antenna beam directly. A typical approximation is to use the 3 dB beamwidth as the resolution capability of the beam. From an extrapolation of Figure 3, it can be seen that an aperture length of 370, 190, and 135 inches is needed at 35, 70, and 95 GHz, respectively, in order to achieve a 1.2 mrad (0.069^{o}) beamwidth. Geodesic lenses in this size range obviously cannot be packaged in the stub-wings. Hence, a technique other than the brute-force method of increasing the aperture size must be used to achieve the desired tracking accuracy. An alternate approach is to use a lens in each wing as an interferometer pair. This approach is considered next.

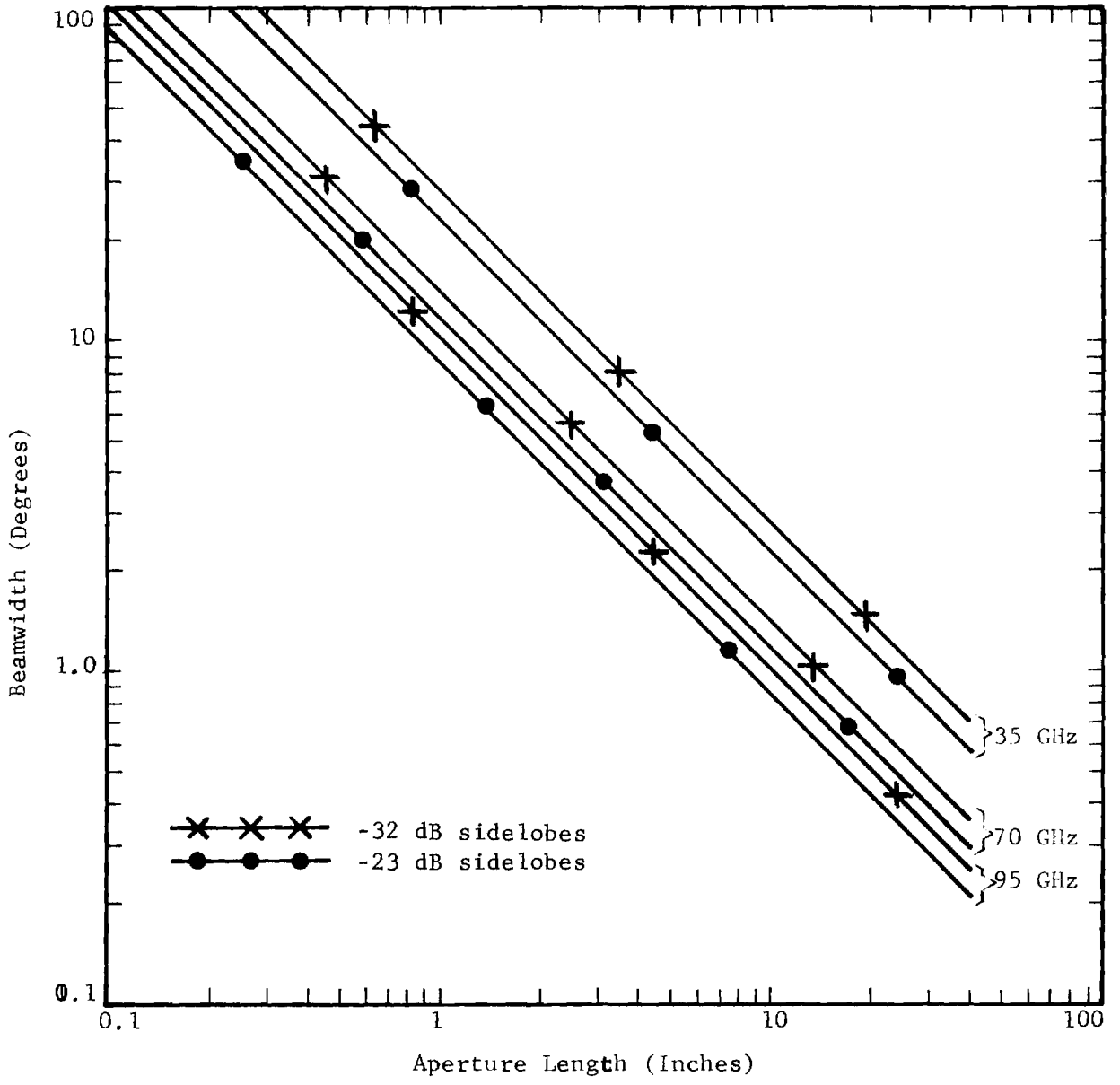

Figure 3. Beamwidth versus aperture length at millimeter frequencies for two different sidelobe levels.

B. Antenna Patterns Produced by Two Antennas Located in the Stub-Wings

An analysis was made of the interferometer effects produced by two antennas (for example, geodesic lenses) located in the stub-wings of the Cobra helicopter. The objective of the study was to determine how much, if any, azimuth beam sharpening could be obtained using the two antennas together. The antennas were modeled as two line sources each of length D and displaced by a distance L as shown in Figure 4. The total pattern will be represented by $E(\theta)$, the array factor by $AF(\theta)$, and the element pattern by $E_e(\theta)$. Thus

$$E(\theta) = E_e(\theta)\ AF(\theta) \tag{1}$$

Assume that Aperture 1 has a complex amplitude A_1 while Aperture 2 has a complex amplitude A_2. Then

$$AF(\theta) = A_1 e^{-jk\frac{L}{2}\sin\theta} + A_2 e^{+jk\frac{L}{2}\sin\theta}$$

Assume a symmetric phase difference of φ between the two elements, and that they have equal amplitudes, chosen to be 0.5 for convenience. Then

$$|A_1| = |A_2| = \frac{1}{2} \quad ,$$

$$\angle A_1 = -\frac{\varphi}{2} \quad , \text{ and}$$

$$\angle A_2 = +\frac{\varphi}{2} \quad .$$

Thus

$$AF(\theta) = \frac{1}{2}e^{-j(k\frac{L}{2}\sin\theta + \frac{\varphi}{2})} + \frac{1}{2}e^{j(k\frac{L}{2}\sin\theta + \frac{\varphi}{2})} \quad ,$$

or

$$AF(\theta) = \cos\Psi \quad . \tag{2}$$

where

$$\Psi = k\frac{L}{2}\sin\theta + \frac{\varphi}{2} = \pi\left(\frac{L}{\lambda}\right)\sin\theta + \frac{\varphi}{2} \quad . \tag{3}$$

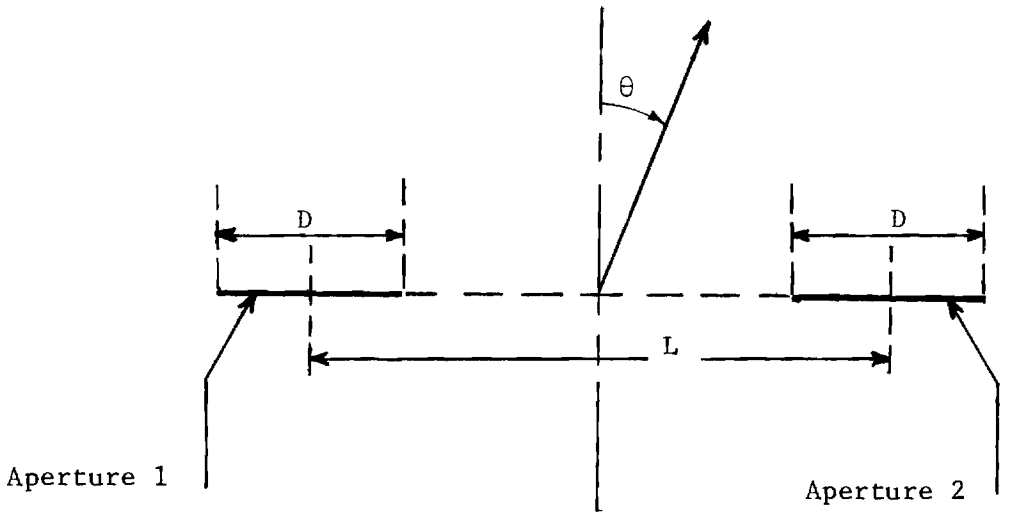

Figure 4. Two displaced, identical antennas.

For ease of computation a simple far field pattern was assumed for the geodesic lens, namely

$$E_e(\theta) = \left[\frac{\sin\left(\frac{u}{n}\right)}{\left(\frac{u}{n}\right)} \right]^n \qquad (4)$$

where n = 1, 2, 3, · · · and $u = \pi(D/\lambda) \sin\theta$. For n = 1 the pattern (4) is produced by a uniformly illuminated line source for which the sidelobe level is -13.2 dB, and the beamwidth is 50.8° D/λ. For n = 2 the pattern (4) is produced by a triangular distribution on the line source for which the sidelobe level is -26.4 dB and beamwidth is 73.4° D/λ.

Patterns were calculated for the following set of parameters:

Lens diameter	D = 25"
Lens spacing	L = 40", 60", 80"
Wavelength	λ = 0.347" (35 GHz), 0.124" (95 GHz)
Phase difference	$\varphi = 0^\circ$
Aperture taper	n = 2 (triangular)

These six patterns are shown in Figures 5-10. A triangular aperture distribution was chosen since it gave reasonable, i.e. -26.4 dB, sidelobes. Note from the figures that the array factor samples the element pattern as expected. Note also that the first interferometer lobe is very high, and is independent of frequency. The level of the first interferometer lobe is tabulated in Table II.

The lenses must be separated by about 70 to 80 inches since the Cobra is 36 inches wide at the wings and the lenses are 25 inches in diameter. Thus, although the main beam of the pattern has been narrowed by using the two antennas as an interferometer, the amplitude of adjacent interferometer lobes are so close to that of the main beam (only about 1 dB down) that it would be impossible to distinguish which lobe was on the target in a tactical situation.

The level of the interferometer lobes can be reduced by decreasing the taper on the aperture since this narrows the main beam. The sidelobe level

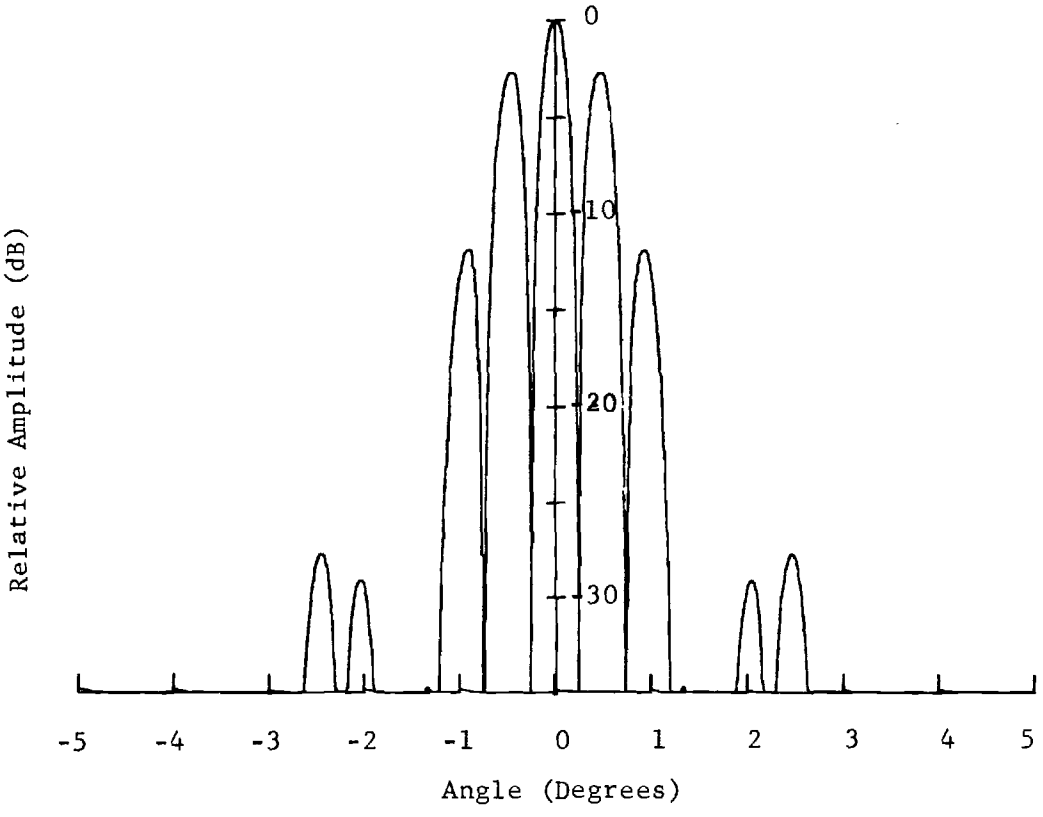

Figure 5. Pattern produced by two line source antennas with D = 25 inches, L = 40 inches, n = 2, and f = 35 GHz.

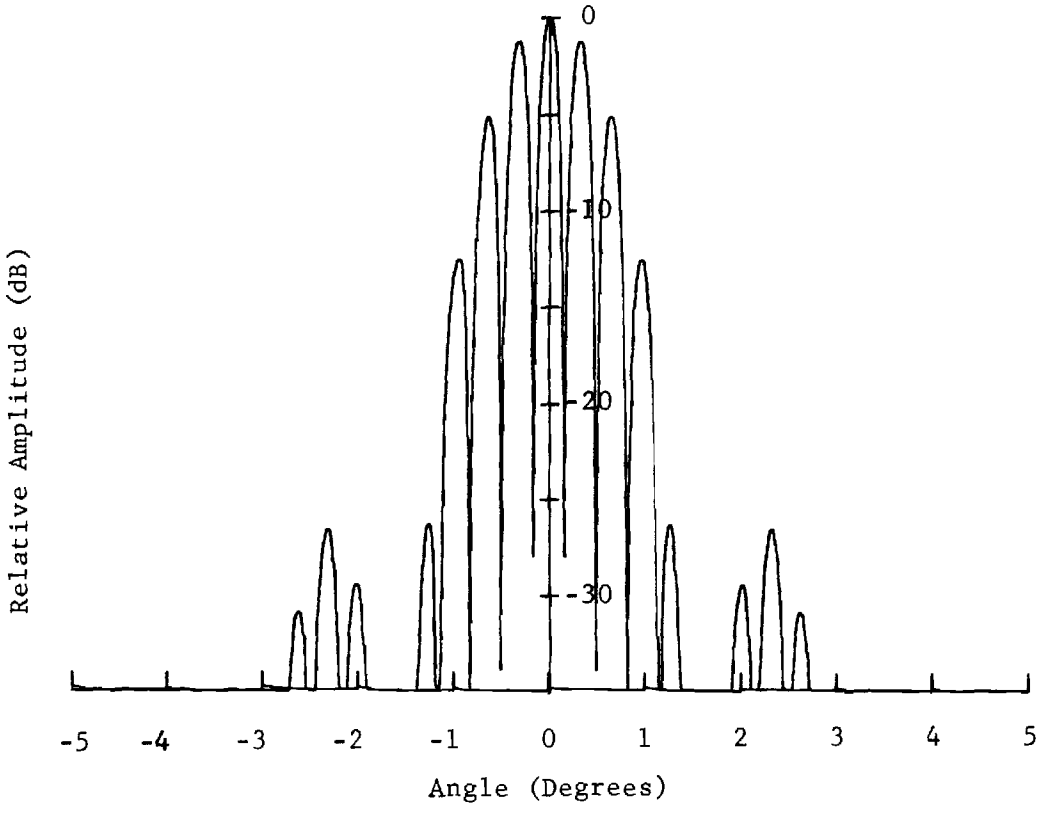

Figure 6. Pattern produced by two line source antennas with D = 25 inches, L = 60 inches, n = 2, and f = 35 GHz.

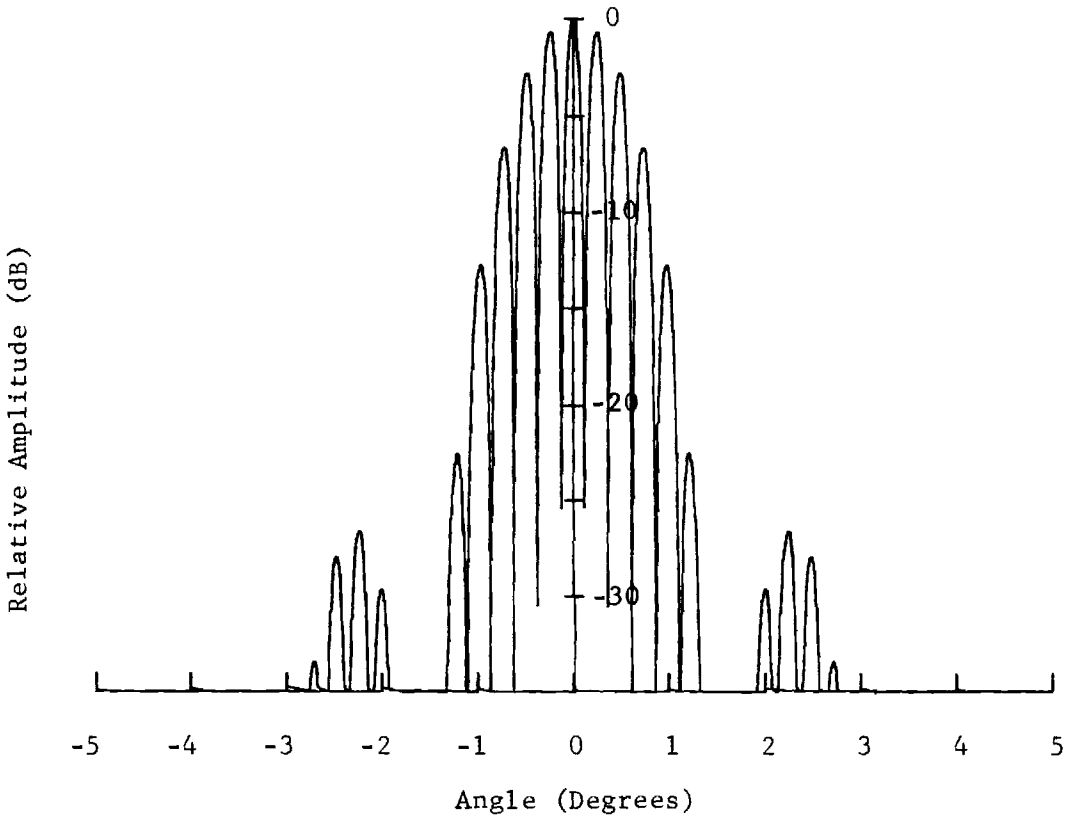

Figure 7. Pattern produced by two line source antennas with D = 25 inches, L = 80 inches, n = 2, and f = 35 GHz.

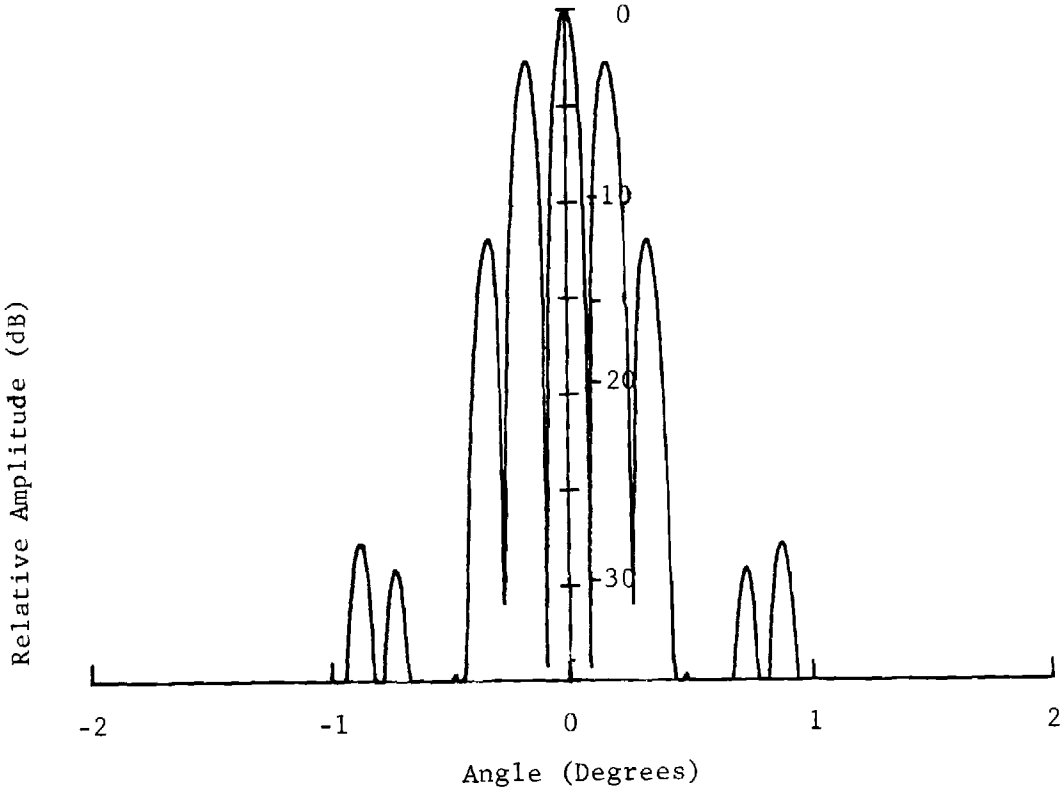

Figure 8. Pattern produced by two line source antennas with D = 25 inches, L = 40 inches, n = 2, and f = 95 GHz.

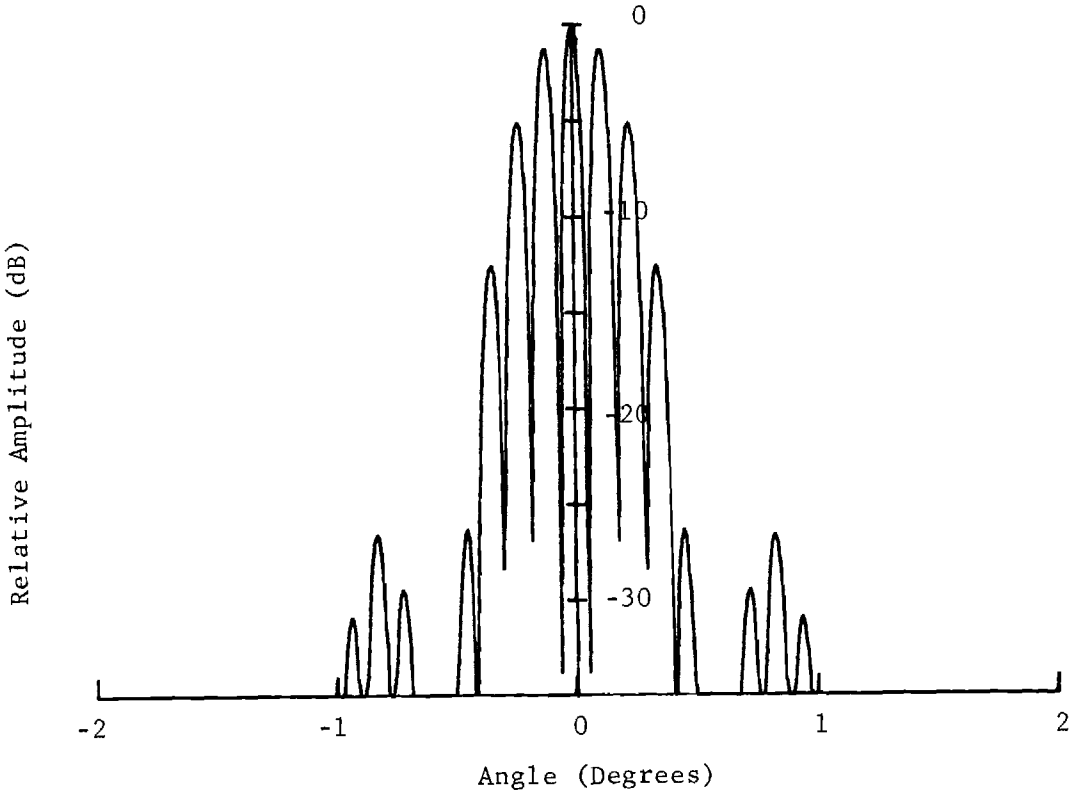

Figure 9. Pattern produced by two line source antennas with D = 25 inches, L = 60 inches, n = 2, and f = 95 GHz.

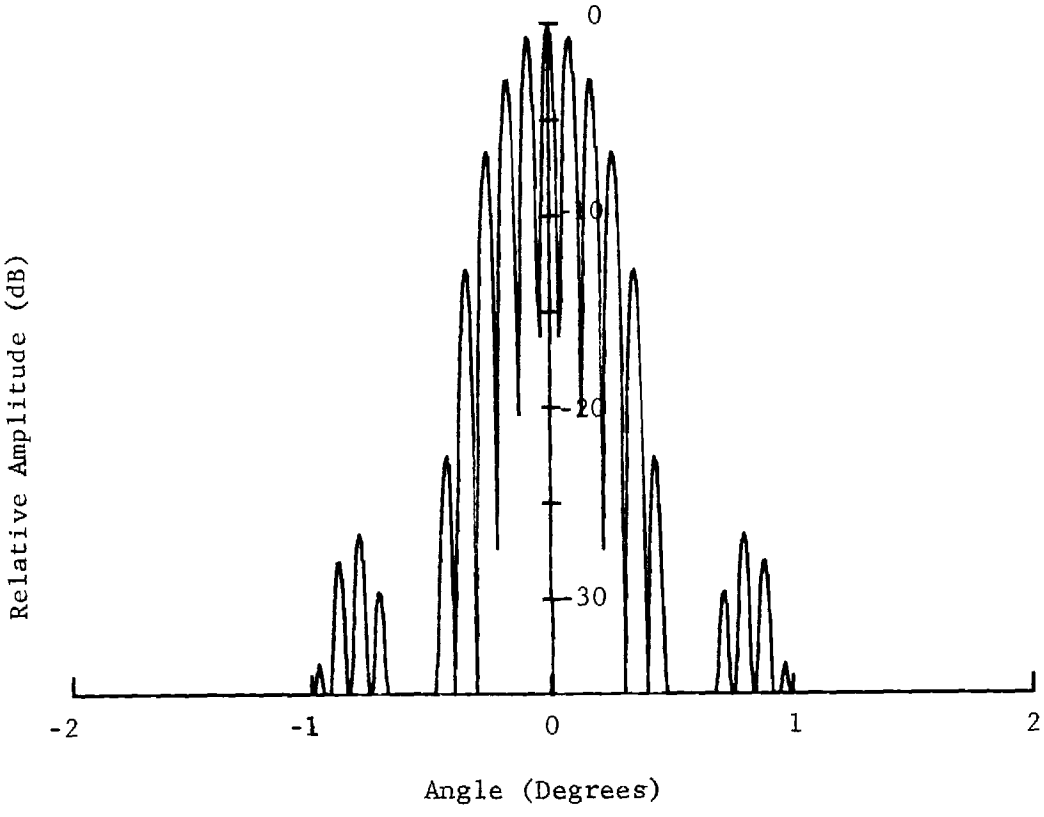

Figure 10. Pattern produced by two line source antennas with D = 25 inches, L = 80 inches, n = 2, and f = 95 GHz.

Table II

Interferometer Lobe Level Versus Separation

L (inches)	First Interferometer Lobe Level (n=2)
40	-2.7 dB
60	-1.2 dB
80	-0.7 dB

of the element pattern is increased, however, by doing this. Calculations for an 80-inch lens spacing and a uniformly illuminated (N=1) aperture showed that the interferometer lobes are only 2 dB below the main beam. Again, the interferometer lobe levels are independent of frequency. Hence, the interferometer lobes are unacceptably high even with a uniformly illuminated aperture.

From the preceding analysis it is concluded that use of a lens in each wing as an interferometer pair will not perform satisfactorily for the leading-edge geometry, since the amplitudes of adjacent interferometer lobes are so close to that of the main beam that it would be impossible to distinguish which lobe was on the target.

C. Monopulse and Conical Scan

Two-plane monopulse tracking was examined for the leading-edge antenna. One concept was to provide a dual mode feed for each geodesic lens for azimuth-plane monopulse and to stack two lenses one above the other to provide elevation-plane monopulse. Such an antenna is conceptually capable of providing dual-plane monopulse; however, an examination of the phase tracking requirements precludes its use at millimeter frequencies. The phase difference between receiver channels must be maintained to within 25° or better for reasonably

proper performance according to Page [8]. Maintaining such tight phase tracking through the lenses, the ring switches and the connecting waveguide of the stacked lens approach would be difficult at 95 GHz, especially while scanning. In addition, it appears that off-the-shelf receiver components at 95 GHz cannot currently provide the required phase stability. Thus dual plane monopulse using stacked geodesic lenses was ruled out. Monopulse could be incorporated in a separate tracking antenna such as the Cassegrain reflector proposed as the result of this study. However, the increased system complexity will still be present since three receivers are typically required for monopulse.

Conical scanning, on the other hand, can be implemented with off-the-shelf receiver components. In addition, its receiver circuitry is considerably simpler than that in monopulse and in many instances the tracking performance of conical scan is as good as that of monopulse. Hence, conical scan is the recommended tracking technique at the present time. As receiver components improve and if ECM conditions require a change, the tracking antenna could be converted over to monopulse at a later date. A rotating subreflector is recommended for producing the conical scan. Such an approach permits a small motor to be used since the mass of the subreflector will be low, and eliminates the need for a rotary joint at the feed.

III. RECOMMENDED ANTENNA GEOMETRY

The results of the preceding sections indicate that the optimum antenna configuration for the 95 GHz modified stub-wing installation consists of three antennas. One geodesic lens will be placed in each wing as shown in Figure 11. Each lens provides 60^{o} of search coverage from dead ahead for a total of 120^{o} search coverage for the antenna system. Data from the two antennas will be combined for presentation on a single display. This will allow the operator to designate (sequentially) targets of interest with a single-cursor system. The conical scan tracking antenna will then be automatically positioned on the designated target and commence automatic tracking independent of helicopter motion. Doppler signature data will be extracted from the track signal to aid in target identification. The tracking information will also be used to cue other sensors and/or for weapons delivery.

The plan view shown in Figure 11 depicts two possible geodesic lens locations. The lower installation depicts the lens attached in front of the present stub-wing of the AH-1G. The upper installation depicts a lens built inside of the present wing. The size of the wing was increased for both installations in order to maintain the same lift to drag ratio as exists in the present wing. The size of the wing is roughly the same for either installation. It should be noted that the stub wings of the Cobra are not aerodynamic lifting surfaces but merely weapon store racks.

The lenses will probably be gimbaled to compensate for aircraft motion. Figure 12 shows the wing size for $\pm 15^{o}$ stabilization in both pitch and roll. The height of the wing appears thicker in Figure 12 than it actually is since it is a front view with the aircraft horizontal and so appears larger in this frontal projection.

Some of the pertinent characteristics of the recommended antenna systems are summarized in Table III. Each 18-inch diameter geodesic lens is connected by parallel plates to a line source feed horn. This horn illuminates a 33-inch long cylindrical reflector that is 4.5 inches high. About 3 inches of the cylinder height is parabolic in shape to produce the non-scan plane main beam while the remaining 1.5 inches is used for beam shaping for short range ground coverage.

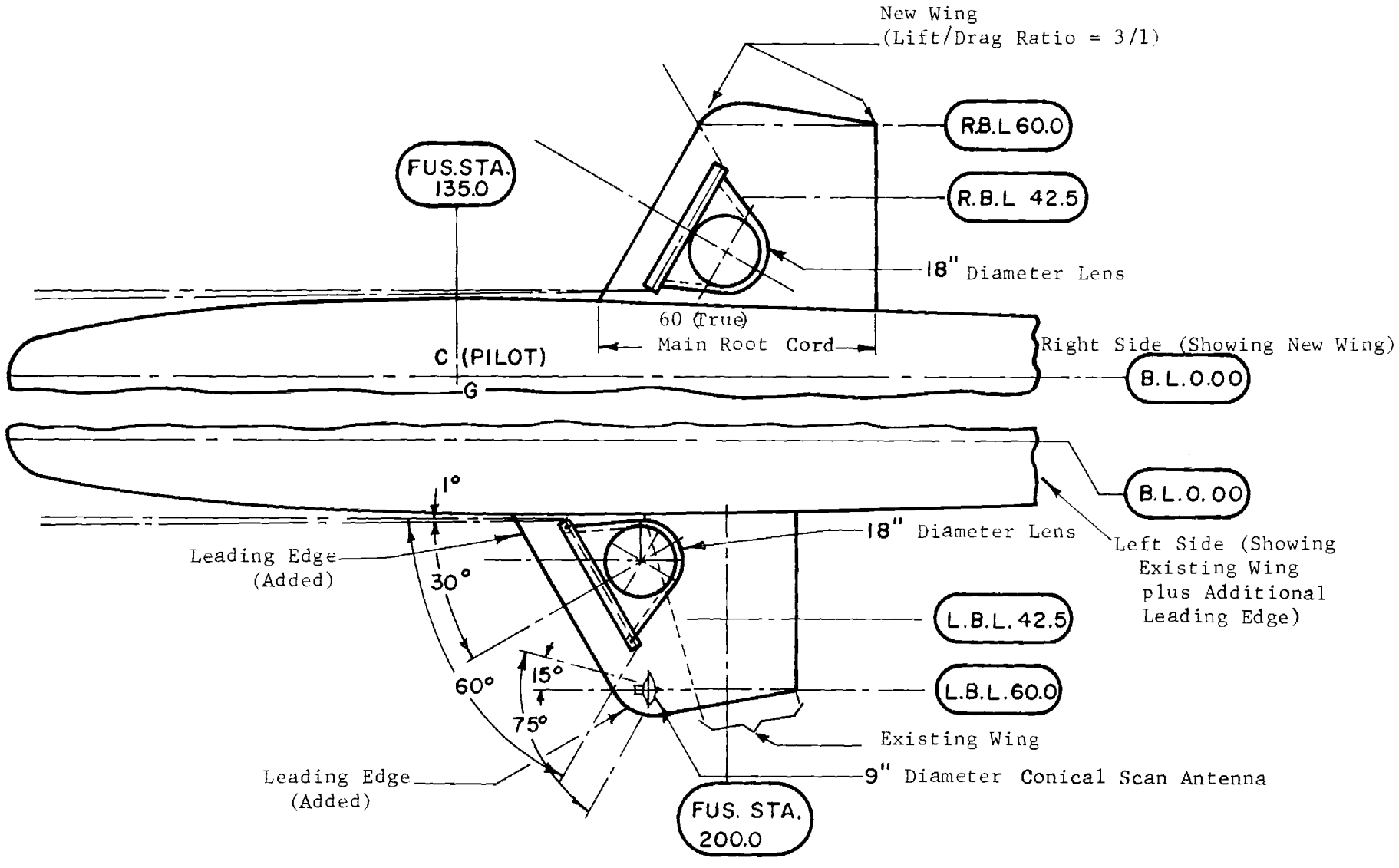

Figure 11. Plan view of stub-wing antenna installation.

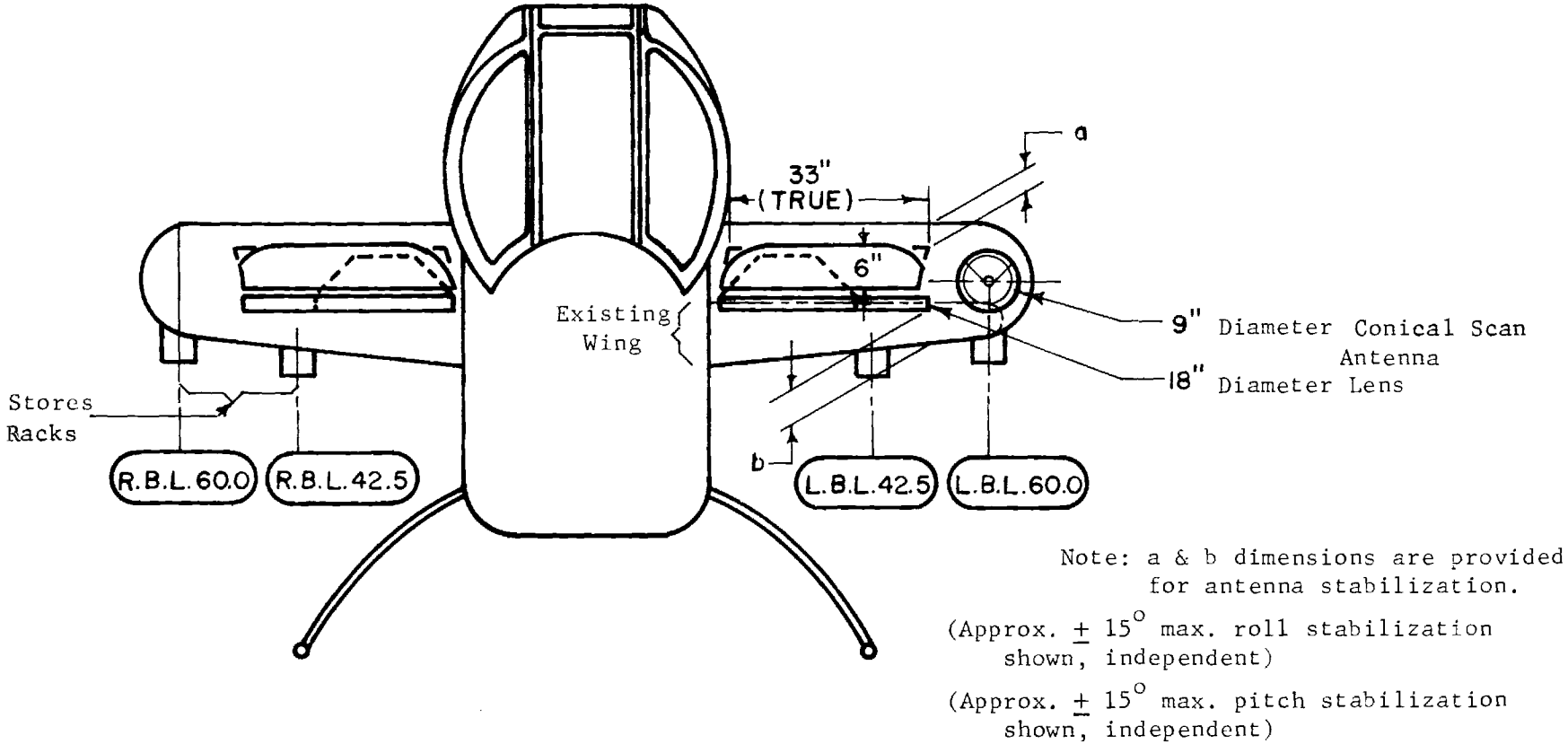

Figure 12. Front view looking aft of stub-wing antenna installation.

Table III

Summary of Characteristics of Recommended
95 GHz Leading Edge Antenna System For the AH-1G Cobra Helicopter

Parameter	Value
Geodesic Lenses (2 each)	
Frequency	95 GHz $\pm$ 2 GHz
Beamwidth (half power)	0.5° Az
	2.0° El plus $\csc^2$ shaping
Scan Sector	$\pm 30^{\circ}$
Sidelobe level	-23 dB wrt main beam
Gain	42 dB
Scan rate	10 scans per second
Power handling	8 kW
Conical Scanning Cassegrain Antenna (1 each)	
Frequency	95 GHz $\pm$ 2 GHz
Beamwidth	1.0° pencil beam
Gain	42 dB
Crossover	-1.5 dB $\pm$ 0.5 dB wrt beam peak
Scan rate	26 rps
Power handling	8 kW

IV. CONCLUSIONS

The findings of the leading edge antenna study for the AH-1G helicopter performed by Georgia Tech under Contract DAAA25-73-C-0648 were reported in the preceding sections. A conceptual design has been obtained for a practical antenna system which can be located in a modified stub-wing of the attack helicopter. The antenna system consists of two 18-inch diameter geodesic lenses and one 9-inch diameter Cassegrain reflector. One lens is placed in each stub wing and each lens scans a 60° sector from dead ahead. Thus, 120° of search coverage is obtained. Target tracking and identification are achieved through the conically scanned Cassegrain antenna located in one of the wings. Since the receiver, transmitter, as well as all other system components are available at 95 GHz, it appears entirely feasible to proceed with the design of a 95 GHz radar for the attack helicopter.

It is recommended that the development of an advanced 95 GHz radar system be undertaken on the basis of the antenna design concepts presented in the preceding sections. It is further recommended that this development be accomplished in four major phases:

I. Antenna Development Program

II. Integrated System Configuration Study and Component Design Validation Program

III. Hardware Feasibility Demonstration

IV. Brassboard/Prototype Development

An outline of these four recommended phases is given below. It is anticipated that an orderly development program, such as one comprising the above would result in a quality radar sensor at minimum risk. The insertion of a low cost, near term, feasibility demonstration radar (Phase III) into the program will provide the Army with a relatively efficient checkpoint to use for an in-depth assessment of the potential of such a new sensor. In addition, this phase will allow for an optimum opportunity for the input of management and technical direction to the development program. A key output of Phase IV will be the detailed technical and management data needed to guide the procurement and production of this system.

Since the antenna subsystem of the radar is a very critical item in determining the radar performance, it is recommended that the antenna be built and tested early in the program (i.e. Phase I). The recommended four phase development program is as follows:

Phase I. Antenna Development Program

Objective: Build and test the two geodesic lenses and one conical scanning antenna specified by Georgia Tech under Contract DAAA25-73-C-0648.

Tasks to be Accomplished: Perform a detailed design, build, test, and deliver the above three antennas. This effort will validate the predictions of performance of the antennas which are very critical items in establishing radar performance.

Phase II. Integrated System Configuration Study

Objective: Define, in detail, the configuration of a 95 GHz radar sensor for use on a scout and/or attack helicopter which is based on the geodesic lens/conscan antenna concept developed by Georgia Tech on Contract DAAA25-73-C-0648.

Tasks to be Accomplished: Examination of the operational requirements, system performance characteristics, detailed subsystem design, clutter reduction techniques, and other signal processing requirements. The results of the detailed examinations above will be merged into a comprehensive system design plan, including specific engineering specifications and design data.

Phase III. Hardware Feasibility Demonstration

Objective: Design, build, and field evaluate a breadboard of the radar system specified in Phase II.

Tasks to be Accomplished: Design and build a breadboard radar operating at 95 GHz which comprises a complete antenna, transmitter, and receiver systems. It will include limited signal processing and simple displays; however, it will be designed to allow the acquisition of calibrated engineering and performance data. A series of ground and flight tests will be undertaken. The resulting data will be analyzed and recommendations (including engineering specifications) will be made for the development of a complete prototype (brassboard) system. The Phase I antennas will be used in this phase.

Phase IV. Brassboard/Prototype Development

Objective: Design, build, and flight test the brassboard radar system recommended in Phase III. The goal is to provide all necessary technical data for use in the specification and procurement of a service approved radar sensor.

Tasks to be Accomplished: Design and build a complete radar including full signal processing and sophisticated displays. Integrate into aircraft, including mating to other sensors, etc. Develop complete test program plan. Support the Army in the performance of comprehensive flight test program. Prepare complete data (software) package. Provide the Army with detailed test analysis, and performance results. Provide the Army with assistance in the preparation of procurement specifications, etc.

REFERENCES

1. Lukes, G. D.,"Penetrability of Haze, Fog, Clouds and Precipitation by Radiant Energy over the Spectral Range 0.1 Micron to 10 Centimeters," Center for Naval Analyses, University of Rochester, Contract No. N00014-68-A-0091, May 1968, AD 847658.

2. Strom, L. D.,"Applications for Millimeter Radars (U)," System Planning Corporation, Contract No. DNA 001-73-C-0098, December 1973.

3. Johnson, R. C., "The Geodesic Luneberg Lens," Microwave Journal, August 1962, pp 76-85.

4. Johnson, R. C., "Radiation Patterns from a Geodesic Luneberg Lens," Microwave Journal, July 1963, pp 68-70.

5. Alford, S. T. et al.,"Microwave Scanning Antenna Studies in Support of Advanced Echo Range Requirements (U)," Final Engineering Report, Prime Contract N00017-62-C-0604, subcontract APL/JHU 271845, Georgia Institute of Technology, June 1973.

6. Long, M. W. and Allen, G. E., Jr., "Combat Surveillance Radar," Final Report on Contract DA 36-039 SC-74870, Georgia Institute of Technology, June 1960, AD 318212.

7. Silver, S., Microwave Antenna Theory and Design, McGraw-Hill, New York; 1948, pp. 177-180.

8. Page, R. M., "Monopulse Radar," IRE National Convention Record, Vol. 3 Pt. 8, pp. 132-134, 1955.

REPORT DOCUMENTATION PAGE

READ INSTRUCTIONS BEFORE COMPLETING FORM

1. REPORT NUMBER	2. GOVT ACCESSION NO. / 3. RECIPIENT'S CATALOG NUMBER
4. TITLE (and Subtitle): 95 GHz Cobra Leading Edge Antenna System	5. TYPE OF REPORT & PERIOD COVERED: Technical Report (Final)
	6. PERFORMING ORG. REPORT NUMBER: EES/GIT Project A-1551
7. AUTHOR(s): Donald G. Bodnar and Robert M. Goodman, Jr.	8. CONTRACT OR GRANT NUMBER(s): DAAA25-73-C-0648
9. PERFORMING ORGANIZATION NAME AND ADDRESS: Engineering Experiment Station, Georgia Institute of Technology, Atlanta, Georgia 30332	10. PROGRAM ELEMENT, PROJECT, TASK AREA & WORK UNIT NUMBERS
11. CONTROLLING OFFICE NAME AND ADDRESS: Frankford Arsenal, Philadelphia, Pennsylvania 19137	12. REPORT DATE: 15 April 1974 / 13. NUMBER OF PAGES: 30
14. MONITORING AGENCY NAME & ADDRESS (if different from Controlling Office)	15. SECURITY CLASS. (of this report): Unclassified / 15a. DECLASSIFICATION/DOWNGRADING SCHEDULE

16. DISTRIBUTION STATEMENT (of this Report)

17. DISTRIBUTION STATEMENT (of the abstract entered in Block 20, if different from Report)

18. SUPPLEMENTARY NOTES

19. KEY WORDS (Continue on reverse side if necessary and identify by block number)

Antenna, Millimeter Radar Antenna, Geodesic lens, Cassegrain antenna, 95 GHz Antenna, Helicopter Antenna

20. ABSTRACT (Continue on reverse side if necessary and identify by block number)

An antenna concept has been developed and a conceptual design performed for a 95 GHz antenna system to be located in a modified stub-wing of an AH-1G Cobra helicopter. The antenna system consists of three antennas: two 18-inch diameter geodesic lenses and one 9-inch diameter Cassegrain reflector. One lens is placed in each stub-wing and each lens scans a 0.5° beam (2° beam in the non-scan plane) over a 60° sector from dead ahead. These lenses provide search coverage over a 120° sector. Target tracking and identification is achieved

by a conically scanned Cassegrain antenna located in one of the wings. Using off-the-shelf receiver and transmitter components, the proposed system should provide detection and tracking out to 12 to 18 km. The existing stub-wing must be approximately doubled in size in order to accommodate the antennas. This wing modification will not significantly alter the aircraft performance since the stub-wing is not an aerodynamic lifting surface.